Design and Testing of a Novel, High-Performance Two DoF Prosthetic Wrist

Revanth Damerla, Kevin Rice, Daniel Rubio-Ejchel, Maurice Miro, Enrico Braucher, Juliet Foote, Issam Bourai, Aaryan Singhal, Kang Yang, Hongju Guang, Vasil Iakimovitch, Evelyn Sorgenfrei, Shorya Awtar

***Abstract*— Extrinsically powered prosthetic wrists have the potential to offer significant improvements to the functionality and dexterity of a prosthetic hand. They can also reduce a user's overreliance on their intact limb and help prevent injury from overuse of upper limb (both intact and residual) and trunk joints. Despite these potential advantages, there are very few prosthetic wrist options that are commercially available and these devices are not commonly used by prosthetic hand users due to several factors including inadequate performance specifications. In this paper, we first seek to establish the target specifications for a prosthetic wrist suitable for both median men and women. We then complete a comprehensive review of the state-of-the-art in extrinsically powered prosthetic wrists in the research, commercial, and patent literature. This review determines that no existing prosthetic wrist meets the target specifications due to the presence of actuators and transmissions that do not offer sufficient torque density, power density, and specific power. In order to address this challenge and produce a prosthesis that achieves target specifications, we next review the performance of existing actuators and transmissions and determine that Brushless DC motors with planetary gearboxes and ball screws offer the best potential to achieve the target specifications. We then present the design of a novel two Degree of Freedom parallel kinematic prosthetic wrist that incorporates this actuator-transmission combination. This first iteration of the proposed prosthetic wrist meets the target torque, speed, and weight but does not meet the target dimensions or range of motion yet. We propose design improvements in subsequent iterations that could lead to a prosthetic wrist that meets all the target specifications of torque, speed, weight, and volume.**

***Index Terms*— Actuators, biomechatronics, mechanical transmissions, physiology, prosthetics**

I. Introduction and Motivation

EXTRINSICALLY powered upper limb prostheses, including prosthetic hands [1]–[8], wrists [9], elbows, and shoulders [10]–[13] have the potential to help the 41,000 amputees missing more than their fingers in the United States [14] and many more worldwide [15]–[17] overcome the challenges associated with upper limb loss. These challenges include efficiently completing activities of daily living (ADLs) and maintaining a sufficiently high degree of independence. For those with limb loss at the wrist (i.e. wrist disarticulation) or more proximally, the prosthesis must ideally comprise an end effector that approximates the functionality of the lost hand as well as the wrist to allow the user to complete ADLs.

Unfortunately, rejection rates for extrinsically powered prosthetic hands without a prosthetic wrist have remained consistently high (>20%) over the past 20 years [18]–[22]. Furthermore, studies have documented that unilateral upper limb myoelectric prosthesis users (i.e. having one intact upper limb and using a prosthetic hand without a prosthetic wrist on the amputated limb) are over reliant on their intact upper limb [23], [24]. One study has shown that 75-94% of upper limb use by a unilateral amputee was with their intact limb [24]. An additional study found that the median use of the intact limb for individuals with unilateral upper limb absence was 79% while the median use of the dominant hand in individuals with two intact upper limbs was 52% [23]. A large proportion of amputees (>50%) have also reported significant pain and injuries to both their intact and residual limbs and other parts of the body including the trunk, neck, and back [25]–[28]. The pain and injuries can come from several sources including phantom limb pain or overuse of joints due to overreliance of the intact limb or compensatory motions of various bodily joints while completing tasks; injuries can include arthritis, joint degradation, muscle injuries, and tendonitis [25]–[28]. These high rejection rates, the overreliance on the intact limb, and prevalence of pain and injuries in amputees are significant because they demonstrate that user needs are not adequately met with current prosthetic hands only (i.e. without a wrist) despite numerous recent technological advancements.

In addition, when both non-users (i.e. people who have rejected extrinsically powered prosthetic hands) and users with transradial (at the forearm) amputations were asked how prosthetic hands could be improved, several answers were consistently given over the past 20 years including reduced weight [19]–[22], [29]–[31], increased comfort of the interface with the user (e.g. socket or harness) [19]–[22], [29], [32], improved controllability and better ease of use [21], [22], [29], [30], [32]–[34], increased durability [20]–[22], [29], [30], [32], and better functionality to enable the user to complete desired ADLs [19]–[22], [29], [34]. Better functionality is related to several specific improvements including increased dexterity (both of the hand and wrist) [22], [29], increased hand strength [32], and increased hand speed [31]. Dexterity requires both the hand and wrist to complete small, precise actions (colloquially called "fine-motor skills") and accurately achieve the desired hand posture or grasp (i.e. have the necessary independently

Revanth Damerla was supported by a National Science Foundation Graduate Research Fellowship during this research. *(Kevin Rice, Daniel Rubio-Ejchel, Maurice Miro, Enrico Braucher, Juliet Foote, and Issam Bourai contributed equally to this work.) (Hongju Guang, Vasil Iakimovitch, and Evelyn Sorgenfrei contributed equally to this work.) (Corresponding author: Revanth Damerla.)*
All authors are with the Precision Systems Design Laboratory, Department of Mechanical Engineering, University of Michigan, Ann Arbor, MI 48109 USA (e-mail: damerla@umich.edu).

controlled Degrees of Freedom (DoFs)).

The prosthetic wrist is a crucial component to addressing the user need of better functionality, particularly increased dexterity, in a prosthetic hand. Just as the human wrist and forearm provide critical articulation that adjusts the orientation of the hand and help it achieve a desired hand posture, the prosthetic wrist can provide the same for a prosthetic hand. Thus, the absence of a prosthetic wrist for prosthetic hand users, even a passively flexible or manually adjustable wrist, can have significant repercussions. Several studies have demonstrated that completing ADLs without a wrist requires significant compensatory motions of both the shoulder and trunk (e.g. leaning to the side) both for prosthetic hands without a prosthetic wrist [35]–[38] and for intact upper limbs with a fused (via a brace) wrist [38]–[40]. As discussed above, compensatory motions can lead to overuse of joints over time that can lead to injuries and pain.

Several studies have also investigated whether a passively flexible [41]–[43] or manually adjustable [43], [44] prosthetic wrist can offer a performance improvement versus no wrist to a myoelectric prosthetic hand user. These studies have not demonstrated improved performance across all tasks. This is not surprising given that these prosthetic wrists are not extrinsically powered and therefore cannot be actively (e.g. myoelectrically) controlled. However, these studies and one survey have consistently found that prosthesis users prefer the functionality and added dexterity of these prosthetic wrists over no wrist [41]–[45]; one study also found that users would have further preferred an extrinsically powered prosthetic wrist [41]. One additional study has investigated the importance of a prosthetic wrist by constraining the number of DoFs of a human hand and wrist in subjects with intact limbs [39]. This study demonstrated that a two DoF wrist capable of Pronation/ Supination (P/S) and Flexion/Extension (F/E) (see Fig. 1) with a 1 DoF gripper performed approximately as well as an intact 23 DoF human hand with a 1 DoF P/S wrist in completing the Southampton Hand Assessment Protocol (SHAP) tasks [39].

These findings demonstrate the importance of an extrinsically powered prosthetic wrist, which can provide the significantly better dexterity users desire in their prosthetic hand, reducing reliance on their intact limb and compensatory motions. This can improve their ability to perform ADLs and also lower the risk of injuries from overuse of joints. However, most commercially available prosthetic hands are not sold with an accompanying prosthetic wrist [3], [8]. There are a few separately sold options for prosthetic wrists [10]–[12], [46]–[51] that typically offer only one (either P/S or F/E) DoF. As discussed above, a prosthetic wrist with more than one DoF provides significantly improved performance over just one DoF and a prosthesis with all three wrist DoFs is necessary to provide sufficient dexterity (see Section IIC). Furthermore, existing prosthetic wrists are relatively heavy and do not offer torque and speed outputs that are comparable with the human wrist and forearm (i.e. inadequate specifications – see Section III). Finally, these options also entail additional cost and complexity. Given this, most prosthetic hand users decide to not include an extrinsically powered prosthetic wrist with their prosthetic hand despite the above-described potential benefits.

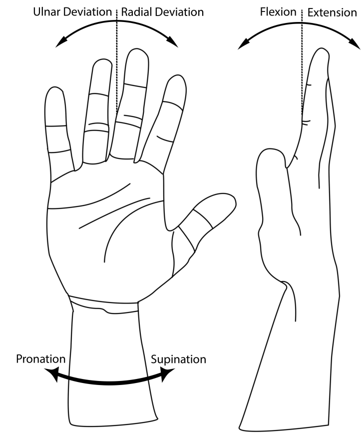

Fig. 1 DoFs of the Human Wrist and Forearm

In this paper, we seek to first understand why commercially available prosthetic wrists have inadequate specifications and secondly to begin to address this challenge with a novel two DoF prosthetic wrist capable of F/E and Radial/Ulnar Deviation (R/U). While the ultimate objective is to provide a prosthesis with all three DoFs (which is necessary to provide sufficient dexterity), the presented prosthetic wrist is an important intermediate step toward achieving this objective. We begin by identifying the target specifications for a prosthetic wrist that can be used by a median man or woman, which are based on the performance of the human wrist (Section II). We then review the specifications of existing prosthetic wrists and show that none of them meet the target specifications (Section III). It is shown that the current gap is mainly due to limitations of existing actuators and transmissions, which cannot provide adequate torque density, power density, and specific power to achieve the target specifications (Sections III and IV). This motivates the design of a new prosthetic wrist that overcomes the limitations of existing prosthetic wrists through the selection of actuators, transmissions, and a mechanism that can achieve the target prosthetic wrist specifications. Next, we review the capabilities of existing actuators and transmissions to identify that Brushless DC Motors with planetary gearboxes and ball screws offer the best potential to achieve the target prosthetic wrist specifications (Section IV). In Section V, we present the design of the novel two DoF parallel kinematic prosthetic wrist. The presented two DoF prosthetic wrist incorporates the above actuator-transmission combination and can achieve the target prosthetic wrist performance and weight but is slightly larger than the target dimensions and does not meet the target range of motion. We also suggest design improvements for how a future iteration of this prosthesis can achieve all target specifications. Finally, Section VI presents the evaluation of a fabricated prototype of the prosthetic wrist to report how well it achieves the desired target specifications.

II. Human Wrist Background

A. Architecture of the Human Wrist and Forearm

The human wrist consists of eight small carpal bones that connect the distal ends of the two bones of the forearm – the radius and ulna – to the proximal ends of the metacarpals in the hand [52]. Together with the radius, ulna, and metacarpals, the carpal bones provide two DoFs through a complex of joints: 1. Flexion and Extension (F/E) and 2. Radial and Ulnar Deviation (R/U) (Fig. 1). The radius and ulna also provide a third DoF – Pronation and Supination (P/S) – by crossing over one another along the length of the forearm [53].

Each of these DoFs is actuated by muscles and tendons housed in the forearm. F/E and R/U are primarily provided by five muscles that originate near the elbow and insert near the proximal ends of the metacarpals [54]. These muscles are located in the superficial layers of the posterior and anterior compartments of the forearm (i.e. near the surface of the top and underside of the forearm). The location of these muscles and tendons produces the highest possible moment arms about the wrist and therefore enables higher joint torques. Actuation for P/S on the other hand is primarily provided by three muscles that originate on the ulna and elbow and insert onto the radius, allowing the two forearm bones to rotate relative to one another [54]. Two additional muscles assist in actuation of this DoF and help stabilize the forearm [54].

B. Human Wrist and Forearm Weight and Dimensions

The mean weight and volume of the hand and forearm for men and women are shown in Table I and are adapted from [8]. Given that a transradial (at the forearm) amputee will have some of their forearm intact, less than half of the weight of the forearm is a logical target for the weight of the prosthesis.

Dimensions of the wrist and forearm are listed in Table II, which were obtained from several studies [55]–[61] that measured these dimensions for U.S. adults with average ages under 30 or people serving in the U.S Armed Forces. As noted previously [8], this may lead to values that reflect people who are younger and more muscular than the typical prosthesis user. In studies that listed the median height and weight of study participants [57]–[60], the median weight of participants in the studies was in some cases over 10kg less than the median U.S. adult while the median heights of participants were within 4 cm of median U.S. adults. This difference in height is significantly smaller than the difference in weight. Thus, length dimensions in Table II are more likely to be representative of the general U.S. population than the width, thickness, and circumference dimensions. However, the wrist is relatively bony and generally lacks significant muscle mass or fatty tissue, meaning these dimensions may still be representative of the general U.S. population despite the difference in weight with participants of the studies. They can therefore still help serve as target dimensions for a prosthesis.

C. Human Wrist Performance

Wrist Range of Motion (RoM) in its 3 DoFs is a critical component of the dexterity it provides and is shown in Table III. While the human wrist can reach certain extreme values in each DoF (denoted as Maximum RoM in Table III) [62]–[67], several studies have measured wrist RoM during completion of ADLs and have demonstrated that the full RoM of the wrist is generally not required (Functional RoM in Table III) [68]–[75]. Since these studies used different ADLs in determining Functional RoM, certain studies found significantly lower values in certain DoFs. These outlier values were removed in order to ensure a representative maximum Functional RoM is listed. Table III illustrates that Functional RoM is substantially lower than Maximum RoM in both F/E and P/S. The Functional RoM also demonstrates the utility of each DoF in completing ADLs. A prosthesis with only one or two DoFs will therefore likely not provide adequate dexterity. R/U in particular is frequently left out of prostheses; while the human wrist has less RoM in this DoF, the Functional RoM demonstrates that articulation in R/U is still valuable.

The maximum joint torque in each DoF is reported for both men and women in Table IV. Studies that measure these values typically measured maximum joint torque in several postures (e.g. wrist fully pronated during a P/S torque measurement) or at several joint speeds (e.g. P/S torque measurement at both 0 °/s and 30 °/s in P/S). Therefore, two separate maximum values are listed for both men and women. True Maximum refers to the maximum value measured in each study across all postures or joint speeds while Mean Maximum uses the mean across all postures or speeds. True Maximum is therefore always higher than Mean Maximum. It is likely acceptable to use the Mean Maximum value in Table IV as a target for a prosthesis as the True Maximum reflects a single orientation or speed that is unlikely to consistently be used in practice.

TABLE I
HAND AND FOREARM WEIGHT AND VOLUME FOR MEN AND WOMEN

	Dimensions	Men	Women
Hand	% Body Weight	0.63 [76]–[79]	0.53 [77], [79]
	Mass of Hand for Median US Adult by Weight (g)	540	380
	Volume (cm^3)	363 [76], [78]	
Forearm	% Body Weight	1.66 [76]–[79]	1.48 [77], [79]
	Mass of Forearm for Median US Adult by Weight (g)	1420	1060
	Volume (cm^3)	909 [76], [78]	

TABLE II
MEAN HAND, WRIST, AND FOREARM DIMENSIONS FOR MEN AND WOMEN

Dimensions	Men	Women
Wrist Thickness (mm) [57], [58]	43.0	37.0
Wrist Width (mm) [55]–[59]	63.1	56.1
Wrist Circumference (mm) [57]–[61]	172.4	149.5
Flexed Forearm Circumference (mm) [59], [61]	307.0	259.1
Radial-Stylion Length (mm) [59], [61]	268.6	242.5

TABLE III
MEAN WRIST AND FOREARM RANGE OF MOTION

Degree of Freedom	Maximum RoM (°)	Functional RoM (°)
Pronation	83 [62]–[66]	61 [68]–[71]
Supination	100 [62]–[66]	75 [68]–[71]
Flexion	76 [62]–[64], [66], [67]	54 [71]–[74]
Extension	73 [62]–[64], [66], [67]	48 [72]–[75]
Radial Deviation	25 [62]–[64], [66], [67]	22 [73]–[75]
Ulnar Deviation	45 [62]–[64], [66], [67]	38 [71]–[74]

TABLE IV
MAXIMUM WRIST JOINT TORQUES FOR MEN AND WOMEN

Degree of Freedom	Men		Women	
	True Maximum	Mean Maximum	True Maximum	Mean Maximum
Pronation	10.3 [58], [84]–[86]	9.0 [58], [84]–[86]	5.1 [58], [85], [86]	4.5 [58], [85], [86]
Supination	10.8 [58], [84]–[86]	9.5 [58], [84]–[86]	5.3 [58], [85], [86]	4.6 [58], [85], [86]
Flexion	14.6 [57], [58], [87], [88]	12.7 [57], [58], [87], [88]	9.7 [58], [88]	8.8 [58], [88]
Extension	9.3 [57], [58], [87], [88]	7.9 [57], [58], [87], [88]	6.8 [58], [88]	5.8 [58], [88]
Radial	14.3 [58]	13.0 [58]	8.8 [58]	8.2 [58]
Ulnar	13.5 [58]	12.4 [58]	8.8 [58]	8.0 [58]

The mean maximum wrist joint speed in each DoF is reported in Table V. Unfortunately, relatively few studies have measured these values. However, three different values are reported for each DoF when available. Peak refers to the maximum instantaneous joint speed that can be measured. Two studies have provided measurements for these values [62], [80]. However, the peak value is substantially higher than what is likely to be used in practice. One study measured the maximum joint speeds in tennis players, which requires relatively extreme maximum joint speeds in all three DoFs [81]. Finally, two studies have measured the joint speeds during practical tasks [82], [83], with one measuring mean joint speeds across many professions [83]. These values provide a reasonable, but lower bound on the speeds necessary to effectively perform ADLs. Two studies have recommended that the maximum joint speed for Flexion/Extension of the fingers of a prosthetic hand be 3.0-3.5 rad/s [1], [2], which can also serve as an upper limit for maximum joint speeds in a prosthetic wrist. Beyond these speeds, controllability can become an issue for prosthetic hand users [3].

D. Target Prosthesis Specifications

Table VI describes the target specifications for the prosthetic wrist design presented below, which are informed by the above values for the human wrist and forearm and the motivation to produce a prosthesis that provides sufficient performance to address the user needs for both median men and women. The prosthesis described in this paper will only provide F/E and R/U and a future iteration will include P/S. The target weight for the prosthesis was set to 260-370 g, 25-35% of the median female wrist to ensure the inclusion of P/S would not lead to an infeasible weight for the intended users. A target width and thickness of 55-60 mm and 35-40 mm respectively were initially chosen. Although these values can be larger than for a median woman, it enables the largest possible space for actuators, transmissions, and other components and is unlikely to prevent a user from completing most ADLs. For example, the median woman's palm thickness at the thenar pad is much thicker – 51.7 mm [55]. Finally, a target length of 70-100 mm was chosen because it is about 30-40% of a median woman's radial-stylion length. This length enables future inclusion of P/S while still being suitable for transradial amputees.

RoM in both DoFs was informed by the Functional RoM, where 25/45 for R/U denotes a 25° RoM in Radial Deviation and a 45° RoM in Ulnar Deviation, leading to a total of a 70° RoM in R/U. A joint torque target of 8-12 Nm was set in both DoFs to provide a sufficiently large percentage of the Mean

TABLE V
MEAN MAXIMUM WRIST JOINT SPEEDS

Degree of Freedom	Peak (rad/s)	Max During Tennis (rad/s)	Mean During Practical Tasks (rad/s)
Pronation	38 [62]	19 [81]	
Supination	33 [62]	5 [81]	
Flexion	27 [62], [80]	17 [81]	1.7 [82], [83]
Extension	26 [62], [80]	8 [81]	
Radial Deviation	10 [62], [80]	3 [81]	1.7 [82]
Ulnar Deviation	11 [62], [80]	15 [81]	

TABLE VI
TARGET PROSTHETIC WRIST SPECIFICATIONS

Weight or Dimension	Value	
DoFs	F/E and R/U	
Weight (g)	260-370	
Width (mm)	55-60	
Thickness (mm)	35-40	
Length (mm)	70-100	
Performance	F/E	R/U
RoM (°)	55/55	25/45
Joint Torque (Nm)	8-12	8-12
Joint Speed (rad/s)	2-3.5	2-3.5

Maximum joint torque for both men and women. This joint torque should be adequate for all ADLs except those requiring more extreme strength such as carrying very heavy objects. A joint speed target of 2-3.5 rad/s was set to exceed mean speeds during ADLs but not exceed what is likely to be controllable for the user. As with the human wrist, the target torque and speed performance are not required simultaneously. Instead, high torque would be required at low speed (i.e. near stall) and high speed would be required while holding relatively small weights.

III. REVIEW OF EXISTING PROSTHETIC WRISTS

In order to develop a prosthesis that meets the above target specifications, it is crucial to understand the specifications of existing prostheses and determine whether any have achieved the target specifications. We have therefore conducted a comprehensive review of the research, patent, and commercial literature. This review builds upon the findings of a previous paper that has reviewed extrinsically powered prosthetic wrists [9] but differs significantly by specifically focusing on each of mechanisms, actuators, and transmissions. These components of an extrinsically powered prosthesis account for the majority of the weight and size and provide its performance.

A. Methods

For this review, a similar process to that used in [8] was used. Extrinsically powered prosthetic wrists described in English and developed between 2000-2021, a period that adequately covers most modern innovations in the field, were identified using several search engines and the following search terms: (“prosthetic hand”, “prosthetic gripper”, “upper limb prosthesis”, “robotic hand”, “prosthetic wrist”) by themselves and in conjunction with the terms (“powered”, “extrinsically powered”, “active”); the references cited by each source were also reviewed to ensure this review examined as many prostheses as possible. The measured specifications of each prosthesis were recorded. In cases where certain values could not be found, the corresponding authors, companies, or creators were contacted to try to obtain the missing values. If the design was never built or if no specifications could be found, the prosthesis was removed from the review as it could not be adequately compared. Prostheses were also removed from the review if newer versions existed, leaving a total of 21 prostheses compiled here.

The specifications of each prosthesis are compiled in Table VII. In several cases, only theoretical values were reported for a prosthesis. These values are not reported in the table because they would imply an efficiency of 100%. Given the high reduction ratios often employed in these prostheses, this assumption is not practical. Losses due to friction, viscous damping, inertia, and other factors can substantially impact performance. For example, the theoretical maximum torque output for the prosthesis reported in [89] is 0.584 Nm. However, the measured maximum torque is 0.0596 Nm, meaning an efficiency of approximately 10%.

An interesting consideration is the total weight of muscle used to actuate the 3 DoFs of the wrist. These values were calculated from the measured volume of each muscle responsible for actuating each DoF from [90]. Unfortunately, this study, which measured muscle volumes for both living men and women, did not list mean muscle volume for men and women separately but provided a single average. However, a different study could not be found providing these volumes in living men and women (and not cadavers) separately. The volumes were converted to weight assuming a muscle density of 1.037 g/cm^3 [91]. Since F/E and R/U are actuated by the same group of muscles, the weight for their actuation was considered together. The muscle weight for P/S includes the brachioradialis muscle, which also aids in flexion of the elbow. The resultant weights can serve as a helpful benchmark for the maximum target weight of the actuators and transmissions used in a prosthetic wrist; the standard deviation can then be used to adjust targets for prostheses meant specifically for either men or women. Ideally however, these components should weigh even less than human muscle to ensure the prosthesis will not be too heavy for the user. For a prosthesis meant for both men and women with transradial amputations, the actuators and transmissions for F/E and R/U each should weigh 50-75g while a P/S module could weigh 100-150g (assuming elbow flexion can be provided by the residual limb or by actuators and transmissions housed in the upper arm for users with

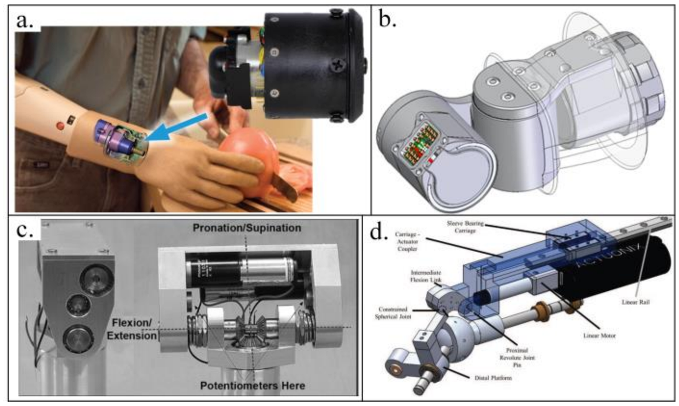

Fig. 2 Examples of Prosthetic Wrists: a. Motion Control Standard Electric Wrist Rotator [46], b. Modular Prosthetic Limb v3 [13], c. Unnamed [98], d. Unnamed [99]

transhumeral or more proximal amputations). While this weight distribution can be altered for a prosthesis with 3 DoFs, 50-75g for each actuator and transmission is a reasonable target for the 2 DoF prosthesis capable of F/E and R/U described in this work. This weight also leaves a reasonable weight for the other mechanical and structural components of the prosthesis.

A final consideration is the type of mechanism used in the prosthesis – serial kinematic, parallel kinematic, or a combination of the two. In the human wrist, F/E and R/U are provided by a parallel kinematic mechanism (PKM) and are connected in serial with P/S. This takes advantage of several aspects of both types of mechanisms. Serial kinematic mechanisms (SKMs) can be simpler, more modular, and have greater ranges of motion than the parallel kinematic options [92]–[94]. However, if both F/E and R/U are provided through a serial kinematic approach, the axes of rotation for these DoFs may not intersect as they do in the human wrist [13]. Currently, no study has been conducted to demonstrate whether non-intersecting F/E and R/U axes are unintuitive for prosthesis users or lead to any loss in performance. PKMs on the other hand can have ground-mounted actuators, can be more compact and lightweight, and potentially have higher speeds, torques, and stiffnesses [92]–[94]. In a prosthesis, the benefits between these two types of mechanisms must be compared while also accounting for the chosen actuator and transmission combination. Given the strict spatial constraints of a prosthesis, specific actuator and transmission combinations may only be feasible with either a SKM or PKM.

B. Prosthesis Review

Eight of the reviewed prostheses provide a single DoF, including four of the five commercially available prostheses. These prostheses were intended for either P/S [46]–[49], [89], [95] (Fig. 2a) or F/E [50], [51], [96], [97]. Of these eight, at least four (but likely more) of the eight prostheses use a Brushed or Brushless DC (BDC or BLDC) Motor connected to a gearbox, whose output directly drives a wrist joint [50], [51], [89], [96], [97]. At least one additional prosthesis uses an ultrasonic motor instead [95]. A common theme among these prostheses is that they often provide at least a functional range of motion, with several P/S prostheses providing a full 360°+

TABLE VII
PROSTHESIS SPECIFICATIONS

Prosthesis Name	Year	#/Type of DoFs	RoM (°)	Serial or Parallel	Width × Thickness (mm)	Length (mm)	Weight (g)	Max Joint Torque (Nm)	Max Joint Speed (rad/s)	Actuator Type	Actuator–Transmission Pathway (Weight (g))
Median Male Wrist		3 (F/E, R/U, P/S)	83/100 – P/S, 76/73 – F/E, 25/45 – R/U	Serial and Parallel	63.1 × 43.0		280-570*	9.0-10.8 – P/S, 7.9-14.6 – F/E, 12.4-14.3 – R/U	38/33 – P/S, 27/26 – F/E, 10/11 R/U	Human Muscle	P/S – Muscle (151±75)-Tendon F/E+R/U – Muscle(153±69)-Tendon
Median Female Wrist					56.1 × 37.0		210-420*	4.5-5.3 – P/S, 5.8-9.7 – F/E, 8.0-8.8 – R/U			
Target Prosthetic Wrist		2 (F/E, R/U)	55/55 – F/E, 25/45 R/U		55-60 × 35-40	70-100	260-370	8-12 – F/E, R/U	2-3.5 – F/E, R/U		
This Design	2021	2 (F/E, R/U)	48/33 – F/E, 33/25 – R/U	Parallel	66 × 52	131.4	$320^{\#}$	8.2 – F/E, 8.4 – R/U	4.2 – F/E, R/U	BLDC	F/E, R/U – Maxon ECX Speed 13L HP (33.7^{+}) – Maxon GPX 13 Speed 25:1 (26^{+}) – 1:1 Spur Gears (8) - Ball Screw + Nut (10) – S-S Link (11)
Motion Control Standard Electric Wrist Rotator (comm.) [46]		1 (P/S)		N/A	47 × 47	70	143	1.7	2.9		
Motion Control Powered Flexion Wrist (comm.) [50], [51]		1 (F/E)	86/67	N/A	46.74 × 46.74	66	258.55	2.3	3.1	BLDC	BLDC – 2-Stage Friction Planetary Drive – 32:3 Evoloid Gear Drive
Ottobock Electric Wrist Rotator (comm.) [47]		1 (P/S)	360+	N/A			96		1.78		
Össur i-Limb Wrist (comm.) [48], [49]		1 – (P/S)		N/A		56	150		1.6		Motor – Planetary Gears
MANUS-HAND [95]	2004	1 (P/S)		N/A						Ultrasonic	Shinsei USR30 (~48) – 10:1 Spur Gears
Unnamed [89]	2012	1 (P/S but with adjustable axis of rotation)		N/A	40 × 40	65	87	0.0596	4.3	BLDC	Faulhaber 0620 K 006 B (2.5) – 5:1 Belt Drive – Faulhaber 08/1K 16:1 (3.8) – 10:1 Pinion and Ring Gears
DTM Wrist [96]	2017	1 (F/E)	90	N/A			175.47		1.0	BDC	MicroMo 1724 006SR (27) – Faulhaber 415:1 gearbox – 3:1 Planetary Gearbox
Unnamed [97]	2021	1 (F/E)	90/90	N/A	43 × 29	37	125			BDC	Dynamixel XM-430-W210-R (105, BDCs – Gears – Mounting Plate)
LUKE Arm (comm.) [10]–[12]		2 (P/S, Combination of F/E and R/U)		Serial							P/S – Motor – Harmonic Drive F/E – Motor – Gears and Non-Backdrivable Clutch
Osaka City University Hand II [100]	2011	3 (P/S, F/E, R/U)	266 – P/S, 175 – F/E, 18.6 – R/U	Serial						DC Motor	P/S, F/E, R/U – DC Motor – Gears
Unnamed [101]	2014	2 (P/S, F/E)	50.4/89.3 – P/S 22.4/41 – F/E	Serial			690			DC Motor	P/S, F/E – Lobot LDX-218 (60, DC Motor – Gears)
RIC Arm [102], [103]	2016	2 (P/S, F/E)		Serial	45 × 35 – F/E Module	58 – F/E Module	378	2.5 – F/E, 2.2 – P/S	7.9 – F/E, 8.7 – P/S	BLDC	F/E – BLDC Motor (26) – Planetary Gear – Non-backdrivable Clutch – Cycloidal Drive
Unnamed [104]	2019	2 (P/S, F/E or R/U)	180 – P/S, 175 – F/E	Serial	74 × 74	118	330	4.3		BDC	P/S, F/E – HiTEC D980TW (79, BDC – Spur Gears)
Modular Prosthetic Limb v3 [13]	2020	3 (P/S, F/E, R/U)		Serial					2.1	BLDC	P/S, F/E, R/U – BLDC Motor – 4:1 Planetary Gearbox – 76:1 Cycloidal Drive
Unnamed [105]	2014	2 (P/S, F/E)	103 – P/S 84 – F/E	Serial	52.8 × 52.8		95.4	0.3209 – F/E		Pneumatic Cylinder	P/S – Pneumatic Cylinder – Rack and Pinion F/E – Pneumatic Cylinder – Link
Unnamed [106]	2009	2 (P/S, R/U)	≥ 60 – P/S, ≥ 20 – R/U	Parallel					~0.56	DC motor	P/S, R/U – DC motors – Spur Gears – Cable + Pulleys
Unnamed [107], [108]	2011	2 (P/S, F/E)	≥ 40 – P/S	Parallel						AC motor	P/S, R/U – AC Motors – Bevel Gear Differential

Unnamed [98]	2011	2 (P/S, F/E)	360 – P/S	Parallel	60 × –	48		0.073 – F/E	4.4 – P/S, F/E	DC motor	P/S, F/E – DC motors – Gears – Bevel Gear Differential
Unnamed [109]	2008	3 (P/S, F/E, R/U)	105 – F/E, 40 – R/U, 95 – P/S	Serial and Parallel						Pneumatic Cylinder	P/S – Bimba 021.5-DXPV – Barrel Cam F/E, R/U – Bimba 022-DXPV/021-DXPV – Link
Unnamed [110]	2008	3 (P/S, F/E, R/U)	70 – P/S, 50/50 – F/E, 30/30 – R/U	Serial and Parallel		≤280				BDC	P/S – Maxon RE 25 (130) – Maxon GP26B (108) – Link F/E, R/U – Maxon RE 25 (130) – Maxon GP26B (108) – Pulleys + Cable
Unnamed [99]	2018	3 (F/E, R/U, P/S)	90 – F/E, R/U 360+ – P/S	Parallel	86 × 86	180	578		1.84 – P/S ≥ 0.6 – F/E, R/U	BDC	P/S - Faulhaber 1717012SR (18) – Faulhaber 15A 249:1 (6) – Belt and Pulleys F/E, R/U – Actuonix P16-50-64-12-P (95, BDC –) – Slider and Rail – Link

* 20-40% of the median forearm weight, + theoretical weights of components – measured total motor + gearbox weight = 63 g, # measured weight without base plate – designed base plate theoretically adds 11 g

rotation. In most cases, the prostheses also meet the minimum target joint speed of 2 rad/s and weigh less than half of the target weight. However, 2.3 Nm was the highest measured joint torque among these prostheses, substantially less than target or anthropomorphic joint torques. These prostheses are also relatively long, making it challenging to connect multiple of them together in series while ensuring the resulting prosthesis is not too long. This is likely a result of the size of the actuator and gearbox, which must be made more compact, torque dense (torque output per unit weight), power dense (power output per unit volume), and have sufficient specific power (power output per unit weight) to meet the target prosthesis specifications. This is the case for the four commercially available 1 DoF prostheses. Thus, most amputees currently have to choose between having no prosthetic wrist, a flexible or manually adjustable prosthetic wrist [9], or a prosthetic wrist capable of only one (but not both) of either F/E or P/S that provides significantly less than anthropomorphic joint torque.

However, six prostheses utilize a motor-gearbox (including spur, planetary, cycloidal, or harmonic gearboxes) combination that is compact and lightweight enough to integrate either two or three of the same (or very similar) combinations serially into a single prosthesis [10]–[13], [100]–[104]. Motor-gearbox combinations that can achieve high torque generally are larger in diameter. For example, the combination for the RIC arm [102], [103] has a maximum width of 45mm. This makes a SKM a logical choice for this combination as it enables each combination to occupy the necessary space without collisions between joints; a PKM would typically require two combinations be able to be housed next to each other, making this actuator-transmission combination impractical. As with the 1 DoF prostheses, which typically utilize similar actuator-transmission combinations, the key challenge for these prosthetic wrists is maintaining both a suitable weight and torque. This is most likely due to the low torque density of most gearboxes (see Section IV). A notable exception may be the Modular Prosthetic Limb (MPL) [13] (Fig. 2b), which takes advantage of the relatively high torque density of cycloidal drives. However, this prosthetic wrist likely does not achieve the target maximum joint torque (target of "near 8 Nm") or prosthesis weight (prosthetic hand and wrist together weigh 1300g).

While PKMs can be lighter weight and produce higher output torques, this does not appear to be the case for the three 2 DoF parallel kinematic prostheses [98], [106]–[108]. Two of these prostheses actuate both P/S and F/E through two AC or DC motors that actuate a bevel gear differential [98], [107], [108] (Fig. 2c). While this leads to a simple and compact mechanical design, bevel gears typically do not provide sufficient torque density to achieve the target prosthesis specifications. Similar reasons most likely limit the third prosthesis, which provides P/S and R/U (but could provide F/E instead) through spur gears that in turn drive cables and pulleys [106].

Three prostheses actuate both F/E and R/U through a PKM, with one actuating P/S serially [109] in a similar manner to the human wrist and the final two actuating P/S through the same PKM [99], [110]. The first [109] actuates F/E and R/U through a RPR+SPS+U PKM, where the prismatic (P) joints are pneumatic cylinders that actuate the two DoFs. Actuation of P/S is provided proximally, through a third pneumatic cylinder that causes a barrel cam to rotate the forearm and wrist. In the second [110], F/E and R/U are provided by two BDCs and planetary gearboxes that actuate cables and pulleys about a spherical joint. P/S is provided proximally by rotating two rods with spherical joints on each end that resemble the radius and ulna. A third BDC and planetary gearbox rotate the two rods about each other via a link to produce P/S. Unlike with the first prosthesis, integrating actuation of P/S into the same PKM means that the actuators providing F/E and R/U are not moved when moving in P/S (an example of ground-mounted actuators). This reduces the inertia required to actuate this DoF, helping to increase maximum speed and torque. The final of these three prostheses [99] (Fig. 2d) is PRS+PSS+S. F/E and R/U are actuated by two linear actuators (the two prismatic joints of the mechanism) composed of a BDC and most likely a leadscrew and nut connecting to distal R-S and S-S links. P/S is provided by rotating a shaft connected to the central spherical joint via a BDC driving a planetary gearbox that in turn rotates the spherical joint via a belt and pulleys. Unlike in the two other prostheses, no part of the forearm rotates due to P/S rotation; instead, only a prosthetic hand connected to the distal end of the prosthesis would rotate, minimizing the inertia that is actuated. Unfortunately, few specifications are provided for these prostheses. While all three are able to provide close to the functional RoM, both [99], [110] are not sufficiently compact.

Furthermore, the weight and joint torque output of [99] do not meet the targets, indicating that a more torque-dense actuator-transmission combination is required. Thus, while PKMs have advantages over SKMs, they require actuators and transmissions that provide significantly higher performance to do so.

A key takeaway from this review is that no prosthesis is currently able to achieve the target specifications of the prosthesis. While several can provide the target RoM and joint speed and be sufficiently lightweight and compact, none have demonstrated achieving the target joint torque while maintaining a sufficient weight. With the possible exception of the MPL [13], the highest measured joint torque is 4.3 Nm [104] (approximately half of the target) in a prosthesis that provides 2 DoFs but weighs 330g (within the target weight) and is significantly larger than targeted. These findings are similar to the current performance limitations of prosthetic hands [8]. The current gap in performance requires an examination of actuators and transmissions to specifically identify those that can offer sufficient torque density, power density, and specific power.

IV. Actuator and Transmission Selection

The human muscle and tendon are a uniquely impressive actuator and transmission, respectively, because they can provide the required torque, speed, and RoM for the DoFs of the wrist at a sufficiently low weight while being packed into a fraction of the overall volume of the forearm. The combination of these attributes makes it very challenging to replicate the human wrist's capabilities in a prosthesis. While many artificial actuator-transmission combinations (with requisite batteries, electronics, etc.) can exceed the performance of human muscles and tendons at larger scales (e.g. automobiles and even prosthetic legs), it is very challenging to meet them while fitting within the limited volume of the forearm.

An actuator and transmission with a rotary output capable of meeting the target prosthesis specifications in Table VI would need to provide an output of 8-12 Nm, 110° RoM, and 2-3.5 rad/s in approximately 75g (based on muscle mass for F/E and R/U – see Section III). Similarly, an actuator and transmission with a linear output would need to provide targets of 270-690 N, 50-86 mm, and 35-105 mm/s, depending on the target joint torque and whether target wrist width or thickness dimensions would provide the limiting constraint. These values correspond to a target specific energy of 300-460 J/kg. The target force and speed output also corresponds to a target stress of 0.85-2.2 MPa assuming the maximum diameter is half the target wrist thickness and a target strain and strain rate of 0.5-0.86 and 0.35-1.05 lengths/s, respectively, assuming the maximum target prosthesis length. In comparison, human muscle can provide a continuous maximum pressure of 0.35 MPa, strain of 0.4, and strain rate of 5-10 lengths/s [91], [111].

Human muscle has a maximum power output at one-third of its maximum force and one-third of its maximum speed capability [91], [111]. The target prosthesis actuator-transmission performance would therefore correspond to a target power output of 1.8-4.7 W, specific power of 24-62 W/kg (continuous specific power for human muscle is typically around 50 W/kg [91]), and power density of 0.025-0.19 W/cm^3. For electromagnetic actuators such as BLDCs, which typically have maximum power output near the maximum force (or torque) and maximum speed simultaneously, the target performance corresponds to a target power output of between 16-42 W, specific power 210-560 W/kg, and power density of 0.23-1.7 W/cm^3. In order to identify whether any existing actuator-transmission combination can provide these target values, critical for producing a prosthesis with the target specifications, we first review existing actuators.

A. *Review of Actuators*

Pneumatic actuators, which include both pneumatic cylinders and artificial muscles (e.g. McKibben actuators), have demonstrated the ability to transmit air pressure greater than 1.4 MPa (200 psi) [112] and can achieve sufficiently high strain rates and specific powers. While pneumatic cylinders can achieve strains greater than the target of 0.5 [112], pneumatic artificial muscles are limited to strains of 0.25 [113] and are therefore infeasible options. However, pneumatic actuators also require a storage tank or compressor and valves, which when combined with the actuators, substantially reduce the specific power and power density of the total system below what is necessary for the prosthesis and also introduce important safety concerns. Precise position and velocity control are also practically challenging, which also limit the dexterity of the prosthesis [113], [114]. These shortcomings cannot be mitigated simply with the introduction of a transmission and have prevented prostheses using these actuators from achieving the target specifications [105], [109].

Shape memory alloy (SMA) actuators are capable of providing sufficiently high stress, strain rate, specific power, and power density [91], [113], [115]–[118]. Despite providing low strains (~0.05), SMAs are small and lightweight enough to fold together several prosthesis lengths of the actuator (as in [119]) and achieve a sufficient stroke. However, SMAs rely on cooling to reach their original shape, and would cause a prosthesis to take several seconds to reach the nominal position (even with an appropriate transmission) and place additional limitations on bandwidth (i.e. limiting the ability to change between wrist postures quickly) and precision [91], [113], [118]. SMAs are also very inefficient compared to most actuators (often less than 5% power efficiency [91], [113], [115]–[118]), meaning that the requisite battery and cooling components to ensure the prosthesis has ideal functionality would substantially reduce both power density and specific power below the target values.

Piezo actuators can offer very large forces, speeds, power densities and specific powers. However, the stroke of these actuators is very small and therefore requires amplification [91]. Commercially available amplified piezos cannot achieve adequate strokes while providing sufficient force, speed, specific power, and power density [120]–[122]. Ultrasonic piezo actuators operate through different principles and thus can achieve sufficient displacements and speeds, but not adequate forces without a transmission [123]. However, electromagnetic actuators such as BDC and BLDC motors are able to achieve higher performance in torque density, power density, and specific power and are therefore better options.

Dielectric elastomeric actuators (DEAs) are a class of particularly high-performance electroactive polymer actuators. DEAs function as capacitors that move based on attraction or repulsion due to applied electric fields. They are typically made of either Very High Bond (VHB) acrylic or silicone-based elastomers and are arranged in two common architectures: spring roll [124]–[127] and stacked [128]–[130]. A key challenge that has limited the practical applications of DEAs of both architectures is that they have a finite maximum work output. Either architecture can achieve relatively large stresses or strains but not both. Thus, when spring roll DEAs were used in an arm wrestling robot, a large number of actuators that required a larger volume than the entire human arm were needed to provide both sufficient force and stroke [125]. The maximum specific energy shown in previous articles [124], [125], [128]–[130] were also not sufficient to meet the target specifications even with a high-performance transmission.

Hydraulically Amplified Self-healing Electrostatic (HASEL) actuators bear some similarities to DEAs and are a relatively new actuator [131]. They consist of a flexible shell filled with a liquid dielectric and an electrode on either side. A voltage applied to the electrodes causes deformation of the shell, leading to a strain. As with DEAs, HASEL actuators have a maximum work output limitation, with an improved version called Peano-HASEL actuators providing specific energy of 35 J/kg. This is only about 10% of the target specific energy and has led to insufficient performance in a prosthetic finger [132]. This performance cannot be improved with the inclusion of a high-performance transmission. However, even though currently insufficient, these actuators do present the potential to provide significant future performance improvements through improved manufacturing techniques that produce smaller pouches (leading to higher forces) and use of materials with higher dielectric constants and breakdown voltages [131], [133]. For example, an approximately 10x improvement in frictional shear stress was previously demonstrated in electrostatic clutches using a similar concept [134]; however, the same materials may not be feasible in Peano-HASELs.

Many other actuators such as magnetostrictive actuators [135], [136], magnetic SMAs [137], [138], and other forms of electroactive polymer actuators [113] have also been developed within the past 20 years. However, none of these actuators (along with required power electronics) have simultaneously demonstrated sufficient force, speed, power density and specific power over adequate strokes in practical applications to provide the target performance. Thus, all the actuators described above will require substantial and disruptive innovations before they can provide the specifications required for a prosthesis. A key conclusion here is that the fundamental limitations of each of the above existing actuators cannot be overcome with a better transmission. Instead, limitations of specific power, power density, or specific energy prevent these actuators from achieving sufficient performance.

Electromagnetic actuators, and more specifically BLDCs, on the other hand, are unique among artificial actuators because they do offer the required capabilities as long as a transmission with certain specifications can be included. BLDCs can achieve sufficient specific powers and power densities in the dimensions and weight of muscles and tendons in the forearm. We have found commercially available BLDCs [139], [140] with values greater than 300-600 W/kg and greater than 5 W/cm^3, respectively. However, the large power outputs of these motors are in a different torque and speed range than what is needed in a prosthesis. BLDCs that can practically fit within the prosthesis and weigh less than 75 g have maximum speed outputs in the range of 8000 rad/s but maximum continuous torque outputs less than 0.07 Nm [139]–[144]. These are much higher speeds and lower torques than the target performance.

For a BLDC to provide the target performance, transmissions that can provide a significant reduction ratio (>100:1) are therefore needed to convert this high-speed, low-torque output into the lower speed and higher torque of a prosthetic hand and wrist. A transmission with sufficiently high torque capability at a low enough weight and size can help achieve the required power density, specific power, and specific work. Therefore, we proceed to review possible transmissions that can be used with BLDC motors.

B. *Review of Transmissions*

Spur and planetary gearboxes are a very common form of transmission, used in at least 13 of the above reviewed prostheses and a large number of prosthetic hands [8]. While they can commonly be purchased already integrated with BLDCs, both types of gearboxes (e.g. [139]–[142]) have poor torque density. For example, the lightest weight commercially available motor-planetary gearbox combinations from Maxon or Faulhaber [139], [140] that could provide outputs of 8 Nm and 2 rad/s (the minimum target performance) weigh approximately 350 g, with the motor only weighing 95 g. While custom gearboxes can produce similar torque outputs for less weight, the large gear face widths needed to produce and transmit such a high torque in a small diameter leads to the large transmission weight; this factor also limits the performance of bevel gears in a prosthetic wrist. However, planetary gearboxes are well-suited for providing the initial reduction from the high-speed, low-torque output of a BLDC to a moderate-torque (~< 0.2 Nm) and -speed output (~< 500 rad/s). This torque and speed range capitalizes on their ability to provide a large reduction ratio while remaining compact and lightweight. For example, the gearboxes selected for the prosthesis presented in this paper provide a reduction ratio of 25:1 through three stages for 26 g, providing theoretical outputs of 0.143 Nm and 264 rad/s. This arrangement has also been used previously in several of the above prostheses.

Harmonic and cycloidal drives offer solutions with even higher torque densities by ensuring many gear teeth are in contact and transmitting torque at the same time (i.e. naturally high contact ratios). However, commercially available options [145]–[149] that can provide at least 8 Nm are infeasibly heavy and are often too large. While the MPL [13] presents cycloidal drives with further optimization that produce higher (but still insufficient) torque outputs, these gearboxes are most likely too

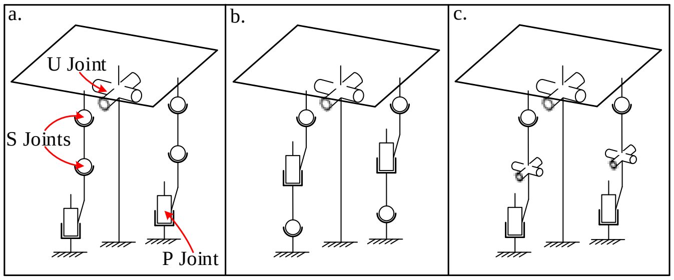

Fig. 3 Examples of 2 DoF Parallel Kinematic Wrists considered: a. 2-PSS+U, b. 2-SPS+U, c. 2-PUS+U

heavy to offer sufficient torque density.

Worm gears are an especially popular solution in prosthetic hands for their non-backdrivability, high reduction ratio, and ability to change the axis of rotation by 90° [8]. While the worm gear is often made of steel and very compact, the wormwheel is typically made of brass or plastic to ensure the pair has sufficiently high efficiency. The low strength of these materials forces the wormwheel to have a relatively large diameter and face width when high torques are required. Thus, the lightest weight commercially available worm-wormwheel pair that can transmit at least 8 Nm was found to be 100 g [150]–[152].

The above review of gear options demonstrates that they are not able to achieve sufficiently high reduction ratios and torque densities to convert BLDC outputs into the target performance without further advances in lightweight, high-strength materials, gears with higher contact ratios, or gear geometries and architectures.

Linkage transmissions offer a solution with a relatively high torque density by taking advantage of the small dimensions of a prosthesis. The corresponding small lengths of the links make them very stiff and capable of transmitting relatively large torques. However, linkages are not able to provide a constant reduction ratio other than 1:1 over a sufficient RoM, preventing them from being the transmission element that converts the output of a BLDC (potentially with a lightweight gearbox) to the target prosthesis performance.

Ball screws are unique because they can transmit small input torques into relatively high forces with very little weight and volume. Given the significantly higher maximum efficiencies of ball screws compared to lead screws (~90% v. 50-60% [153]–[157]) for sufficiently lightweight options, we only consider ball screws in this discussion. For example, 4 mm diameter ball screws are capable of transmitting up to 790 N [153] and will not theoretically buckle under this load or the corresponding required speed because of the relatively small required stroke (and therefore small ball screw length) for the prosthesis. Furthermore, the small length of the ball nut means that strains of 0.8 are feasible. These ball screws are available with leads down to 0.5 mm, which would turn 0.024 Nm into 270 N assuming 90% efficiency (~33:1 reduction ratio when converted to 8 Nm). This torque is even small enough to be provided directly from a BLDC without any gearbox. Most importantly, this performance can practically be provided for just 10g, as in the prosthesis presented in this paper.

At the scale and target weight of the prosthesis, we have found no transmission option, other than ball screws, that is capable of generating a sufficiently high force or torque from a BLDC with a gearbox. Other commonly used options such as belt drives [158], lead screws [159], and chains [158], [160] do not simultaneously provide comparable reduction ratios, weights, and output torques to compete with gearboxes at lower torques or with ball screws at higher torques. Unlike any other transmission option, ball screws can therefore enable BLDCs with gearboxes to achieve sufficiently high torque density, power density, specific power, and specific work in the prosthesis.

V. Prosthesis Design

A. Mechanism, Actuator, and Transmission Selection

Among the commercially available BDCs and BLDCs [139]–[144], planetary gearboxes [139]–[142], and ball screws [153]–[157] considered, the lightest weight combinations capable of providing at least the minimum required force and corresponding minimum speed are Maxon BLDCs and planetary gearboxes [139] combined with KSS ball screws [153]. However, the dimensions of the feasible Maxon BLDCs and gearboxes, which are sold integrated as a single unit, have diameters under 16mm and lengths greater than 75mm (i.e. thin and long). These dimensions make it impractical to stack multiple of these BLDCs, planetary gearboxes, and ball screws serially in an SKM while maintaining the target dimensions and RoM (Table VI). Options with shorter and stockier aspect ratios are not viable because they are substantially heavier.

However, PKMs can incorporate ground-mounted actuators and are better-suited to integrate long and thin BLDC + gearbox combinations. Among the several considered 3 DoF parallel kinematic wrists from the literature [9], [92], [161], we were unable to devise one that had a sufficient RoM and aspect ratio conducive to achieving the target specifications while integrating the Maxon BLDCs and planetary gearboxes. We therefore evaluated existing 2 DoF PKMs that could provide F/E and R/U. A future iteration of this prosthetic wrist will include P/S, which is critical to a prosthetic wrist that meets user needs (see Section IIC). P/S could be provided serially and connected proximally to the presented prosthesis (possibly via a different transmission pathway) in a similar fashion to [109], [110] and the human forearm and wrist.

When selecting a 2 DoF parallel kinematic wrist, several critical requirements were considered. The mechanism needed to include prismatic (P) joints in order to accommodate the BLDCs, planetary gearboxes, and ball screws, which have linear outputs. The mechanism also needed to provide sufficient load bearing and transmission capabilities, mechanical advantage, RoM, and aspect ratio to achieve the target specifications. A mechanism with a stationary center of rotation in displaced configurations was also desirable as it would be more like the human wrist and therefore more intuitive for the user to control. Among the numerous existing 2 DoF parallel kinematic wrists [9], [92], we found that PKMs consisting of a single central chain providing at least two DoFs (e.g. via a universal (U) or spherical (S) joint) and at least two actuating chains that incorporate a P joint (e.g. PSS, SPS, PUS) met these requirements (see Fig. 3).

The 2-PSS+U mechanism (Fig. 3a) [92] was ultimately chosen because each joint offers specific functions ideal for their locations within the mechanism. By ensuring the P joint in the actuation chain is most proximal (in contrast to in an SPS chain), the stators of the BLDC and gearbox do not have to move, thereby reducing the mechanism's actuated inertia, width, and thickness. Spherical joints were selected in the PSS chain (e.g. as opposed to PUS or PRUU) despite engineering challenges such as slop and limited RoM because they can compactly provide the load transmission capability. Since these chains are on the outside of the mechanism, compact spherical joints can lead to a larger lever arm and therefore smaller required output force from the actuator and transmission. However, a U joint was chosen for the central chain because it can provide a larger RoM and adequate load bearing and transmission capabilities despite being larger. Since the central chain is responsible for providing the constraints within the mechanism [92], the lower slop of the U joint is an additional advantage. The U joint also has axes of rotation that intersect, ensuring the center of rotation of the mechanism is stationary in all displaced configurations.

The chosen mechanism is also very similar to the human wrist. The wrist joint is kinematically modeled as a universal joint while the four muscles that actuate it are located on the outside of the forearm and are functionally similarly to actuated prismatic joints. The tendons that serve as the transmission connecting the muscles and wrist joint are analogous to cables and have a similar function to the spherical joints (together called an S-S link). The key difference between them is that tendons are only semi-rigid in tension while the link connecting the spherical joints in the S-S link is rigid in tension, compression, and bending. This reduces the number of actuators from four muscles for a human to two BLDCs for the prosthesis and therefore also reduces the required power density, torque density, and specific power. However, the ability of tendons to bend (i.e. low bending stiffness) helps to increase the RoM of the human wrist and maintains a higher mechanical advantage in displaced configurations (e.g. fully flexed) compared to the 2-PSS+U mechanism. An S-S link with finite bending stiffness could therefore offer potential performance improvements that will be explored in future research.

After selection of the 2-PSS+U mechanism, the Maxon ECX Speed 13L HP BLDC, Maxon GPX 13 Speed 25:1 Planetary Gearbox, and KSS SR0402-C7 ball screw and nut were found to be the lightest weight actuator and transmission combination capable of providing the target speed and torque. The BLDC's listed maximum continuous torque is τ_m = 0.00715 Nm and maximum continuous speed is ω_m = 6600 rad/s. The planetary gearbox has reduction ratio N_g = 25 and theoretical efficiency η_g of 80% (reasonable for Maxon 2-stage planetary gearboxes [139]), providing an output torque and speed τ_g and ω_g of:

$$\tau_g = \tau_m \eta_g N_g = 0.143\ Nm, \omega_g = \frac{\omega_m}{N_g} = 264\ rad/s$$

The gearbox outputs are converted by the ball screw, with lead ℓ_b = 2 mm and η_b of 80% (conservative for KSS ball screws

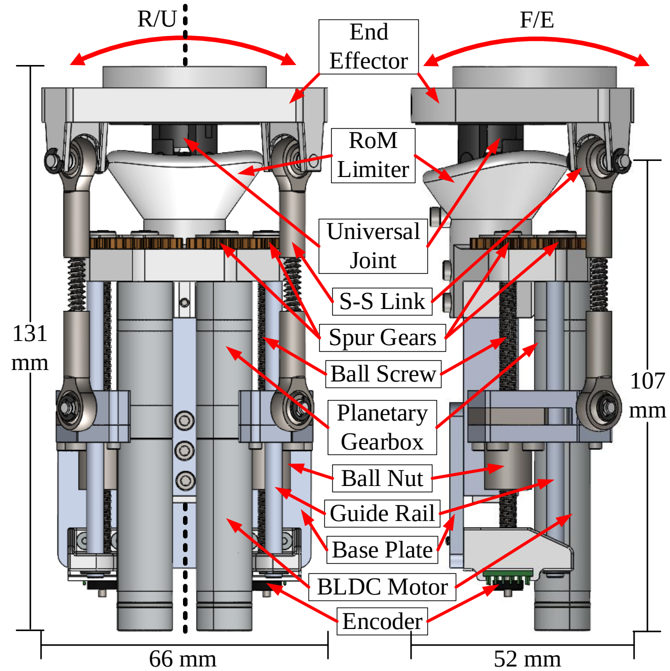

Fig. 4 Prosthesis Design: Top view (left), Side view (right)

[153]), to an output force and speed F_b and v_b of:

$$F_b = \frac{2\pi\tau_g\eta_b}{\ell_b} = 360\text{ N}, v_b = \frac{\omega_g\ell_b}{2\pi} = 85\text{ mm/s}$$

Assuming a lever arm of r_w = 27 mm, 45% of the maximum target wrist width (to account for the width of a S-S link), this corresponds to prosthesis maximum continuous output torque and speed τ_w and ω_w of:

$$\tau_w = r_w \times F_b = 9.7\text{ Nm}, \omega_w = \frac{v_b}{r_w} = 3.1\ rad/s$$

in the nominal position; both are within target performance.

B. *Detailed Design Overview*

Fig. 4 illustrates an overview of the prosthesis design. The prosthesis from the top view (left) is symmetric about the illustrated dashed black vertical center line except for the *universal joint.* It is therefore possible to rotate the wrist 180° about this line, swapping Flexion with Extension and likewise Radial and Ulnar Deviation. The prosthesis is oriented such that the *End Effector* is the most distal component from a user's elbow (see Fig. 5). The *End Effector* could include an integrated interface (e.g. [162]) that would connect to a prosthetic hand. The space around the *universal joint* is also available and could be used to allow wires necessary to power and control the prosthetic hand to pass through easily without sharp bends. Finally, the prosthetic wrist could be secured to the user through a socket or connect to more proximal prosthesis components such as a P/S prosthetic wrist or prosthetic elbow via a rigid connection to the *base plate*.

Actuation in both DoFs is provided by the two *BLDC motors* (as seen in Fig. 4), each connected to a *Planetary Gearbox*. The output shaft of each *gearbox* is connected to a *spur gear* via a shaft coupler. Each *spur gear* drives a second *spur gear* that is in turn coupled to a *ball screw*. Rotation of each *ball screw* drives the linear motion of a *ball nut*, which is constrained to translate by a *guide rail*. Each *ball nut* is also connected to an *S-S Link*; the *S-S Links* are also connected to the *End Effector*, which is constrained to rotate in F/E and R/U by the *universal joint* in the center (and forming the 2-PSS+U mechanism). Thus, F/E is provided by driving the *BLDCs* such that both *ball nuts* translate in the same direction (both up or both down in Fig. 4). R/U is provided when the *ball nuts* are driven to translate in opposite directions (one up and one down in Fig. 4).

A significant consequence of the actuator and transmission selection is that the total length of the *BLDC*, *planetary gearbox* (including output shaft), and *ball screw* is 168 mm. Given the maximum target length is only 100 mm, the *ball screw* must be kept parallel and next to the *BLDC* and *gearbox* instead of being collinear (as would be possible with a shorter BLDC and gearbox). We therefore selected lightweight pairs of brass *spur gears* (SDP/SI A 1B 2MYK08020), modified to reduce the face widths and remove the hub. The resultant mass of each pair of *spur gears* was 8 g (4 g per gear), which is inconsequential to the actuator and transmission selection.

However, not keeping the *BLDC* and *gearbox* collinear to the *ball screw* leads to the prosthesis' larger than target dimensions. Spatial constraints in both width and thickness caused by the *BLDCs* being placed parallel to the *ball screws* and *S-S links* lead to the prosthesis being wider and thicker than targeted (66 × 52 mm rather than 55-60 × 35-40 mm). Furthermore, the *BLDC* and *gearbox* protrude further than any other component on the proximal side of the prosthesis and therefore dictate the prosthesis' length (131 mm rather than 70-100 mm). However, the practical length of the prosthesis is shorter than the measured length. The center of the *universal joint* is the location of intersection of the DoFs of the wrist [92] and the prosthesis would be positioned such that this location coincides with the virtual center of the human wrist (as shown in Fig. 5). Thus, the *End Effector* and distal half of the *universal joint* could be integrated into the prosthetic hand and the prosthetic wrist would only need a length of 107 mm in the forearm.

The aluminum shaft *guide rails* run parallel to each *ball screw* to constrain the *ball nut* to translate and to absorb any potential radial load, which the *ball screw* and *nut* are not rated for. An Oilite bushing serves as the linear bearing connecting the *guide rail*, *ball nut*, and *S-S link* via aluminum plates. The *ball nut* is only constrained to these components along the *ball screw* direction of travel (vertically in Fig. 4). Undersized shoulder bolts secured to the aluminum plates ensure the *ball nut* can float in the other two directions (right/left and into the page in Fig. 4) and isolate it from radial loads. This approach for a *guide rail* is different from that used in [99], which uses commercially available precision guide rails and sliders. While precision guide rails and sliders are more efficient, they are significantly larger and would prevent the prosthetic wrist from meeting target dimensions (as in [99]). More compact, circular linear bearings such as those used in many 3D printers were also considered but options that were sufficiently compact were not found because of the spatial constraints caused by the non-collinear *BLDC*, *gearbox*, and *ball screw*.

Spherical joint selection was primarily dictated by RoM. While the required RoM for the joints of the *S-S link* are not as large as the RoM of the central *Universal Joint*, the RoM of the selected spherical joints (59935K14 – McMaster-Carr, USA) is a relatively small swivel angle of 30°, the highest found among sufficiently compact spherical joints. RoM of the prosthesis is therefore currently limited by these components, which is enforced by the *RoM Limiter* (i.e., mechanical hard-stop). In the future, custom-made spherical joints with larger RoM (e.g. [163], [164]) could be used to ensure the prosthesis RoM meets the target values. The selected *Universal Joint*, the RS Pro 7906699 Universal Joint, is the lightest weight option that was found with ample load rating and RoM. It has a torque transmission rating of 600 Nm, which theoretically translates to an axial load rating over 1 kN.

Fig. 5 Prosthesis without wires and base plate overlaid on an approximately median male wrist and forearm extending to the elbow on the right

Fabrication of the prosthesis was primarily carried out using traditional fabrication techniques on a mill and lathe. Several additional components including the *End Effector*, components mounting the *motors* and *ball screws*, *RoM Limiter*, and shaft couplers were 3D-printed using the Formlabs Form 3 and UV-cured Rigid 4000 Resin, a high-strength plastic resin. The *ball screws* were cut to length and modified to have custom journal ends on a manual surface grinder because they are made of a hardened carbon steel (SCM415) that could not be machined on a lathe with carbide insert tooling.

VI. Prosthetic Wrist Evaluation

The prosthesis is shown without its wires and base plate overlaid on an approximately median male wrist and forearm in Fig. 5 to demonstrate its relative size. The fabricated prosthesis includes an integrated prosthetic gripper not presented in this paper (see Fig. 6), which shares a common, larger base plate than that illustrated in Fig. 4. The measured prosthesis weight of 320 g listed in Table VII therefore does not include this weight, which would theoretically lead the prosthesis to weigh 331 g. Given the presence of this prosthetic gripper, the prosthesis was operated with the End Effector mounted into a vice and the rest of the prosthesis moving (i.e. backwards to how it is presented in Fig. 5, as shown in Fig. 6). The total moving weight during evaluation is therefore approximately

600 g, a representative weight for if the prosthetic wrist was oriented as intended and articulating an average prosthetic hand (that would be attached to the End Effector) holding a lightweight 100-200 g object.

RoM was measured via still images of the prosthesis positioned in the four extreme angles using Adobe Photoshop 2021. The differences in RoM between Flexion and Extension (48°/33° in F/E) and Radial and Ulnar Deviation (33°/25° in R/U) can be attributed to the functionality of a universal joint. The first of the joint's two rotations is about a fixed axis relative to ground while the second is about an axis that rotates about the first axis. This places different limits on the RoM of the S-S links' joints in Flexion versus Extension and similarly for R/U. The axes of the universal joint were therefore positioned to maximize Flexion, which has the largest Functional RoM. The prosthesis surpasses the target Radial Deviation (25°) and is within 15% of the target Flexion (55°). However, further improvements to the RoM of the S-S link spherical joints (as has been demonstrated previously [163], [164]) will be needed to achieve the target RoM in both directions of each DoF.

For speed and torque evaluation, the *BLDCs* were each individually current driven by an Advanced Motion Controls AZB10A4 PWM servo drive and MC1XAZ02 mounting card, each individually powered by a MeanWell LRS-75-24 24V DC power supply and controlled simultaneously by a single NI myRIO operating NI LabVIEW. Position feedback of each *ball screw* is provided by 12 CPR magnetic *encoders* (Pololu 3081), with encoder wheels press fit onto one end of each *ball screw*.

Maximum speed in F/E and R/U without any additional loads applied to the prosthesis beyond the 600g moving mass (representative of a prosthetic hand holding a small weight) were measured individually from video footage recorded on an Apple iPhone 10 at 30 fps (see Supplementary Video 1). For measurements in F/E, a current impulse was sent to move the prosthesis from fully flexed to fully extended and vice versa; analogous measurements were conducted in R/U. The change in angle between frames was measured using Adobe Premiere Pro 2022 to calculate the maximum speed. The prosthesis achieved a measured maximum speed of 3.1 rad/s at the nominal configuration and 4.2 rad/s at displaced configurations, meeting or exceeding the target speed range of 2-3.5 rad/s. In order to evaluate the prosthesis' performance in both DoFs, the prosthesis was commanded to trace a cone at a set frequency. The prosthesis was able to trace a cone with a 23° angle from vertical at a frequency of 1.5 Hz (see Supplementary Video 1).

Maximum torque output was measured while the prosthesis was not moving (i.e. stall torque while articulating 600g) by securing a Yo-Zuri SuperBraid 50 lb. Braided Fishing Line tied to the prosthesis on one end and on the other to a TAL220 10 kg straight bar load cell bolted into a rigid plank secured in a vice (Fig. 6). The load cell measurements were recorded on an Arduino Uno from a HX711 Sparkfun Load Cell Amplifier connected to the load cell. Before measurements were taken, the load cell was calibrated using standard weights. Lever arms were measured using digital calipers. Before each joint torque measurement was completed, the prosthesis was positioned in the nominal position, the cable was slack, and the load cell had

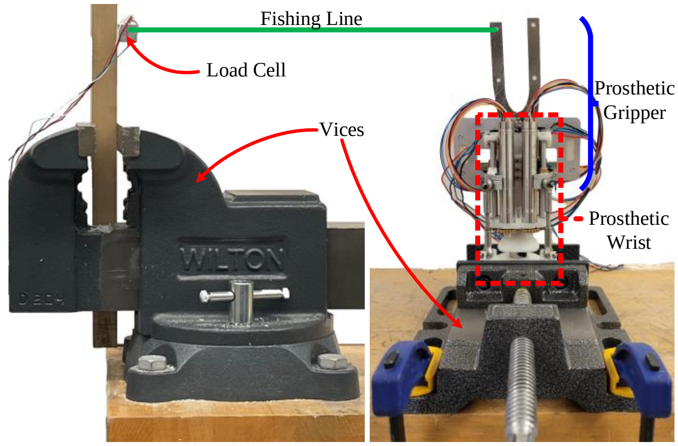

Fig. 6 Evaluation Setup for Maximum Torque Output Measurement

a measured force of under 20 g. A current impulse was commanded and held for at least 2 s and the maximum measured force was recorded. When the commanded current impulse was the continuous rated current of 2.2 A for the BLDCs, the torque was measured to be 7.0 Nm in R/U and 7.5 Nm in F/E. However, the BLDCs were not appreciably hotter than previously, demonstrating that the maximum torque output is higher for at least a period of 2s. Current impulses up to the power supply current rating of 3.2 A were provided, leading to the measurements of 8.4 Nm in R/U and 8.2 Nm in F/E listed in Table VII. This is therefore the first prosthetic wrist to exceed the minimum target joint torque of 8 Nm. However, the BLDCs were still not appreciably hotter after these current impulses and even higher torques could possibly be achieved. This could be applicable in brief tasks the user may perform when larger torques are required (e.g. short-term heavy lifting).

The substantially lower measured torque values at the rated continuous current of the BLDCs (compared to the theoretical value of 9.7 Nm) indicates that the mechanism is not as efficient as initially designed. While the efficiency of the planetary gearbox or ball screws and nuts could be lower than predicted, it is likely that this reduced efficiency is from other sources. These sources could include the spur gears but is more likely to be from the Oilite bushings used as the linear bearings for the guide rails. These bushings will be replaced with more efficient bearings in future versions of this prosthesis.

The combined weight of the actuators and transmissions excluding the S-S links (which are analogous to tendons in function) is 162 g. This is comparable to the weight of the muscles that actuate F/E and R/U in the human wrist (153 g ± 69 g). While the prosthesis cannot achieve True Maximum male joint torques, a heavier and larger prosthetic wrist (feasible for a median male) with larger BLDCs and planetary gearboxes could supply adequately high torque outputs. However, despite the high torque and speed performance of this prosthesis, which is the first to meet both target values, this actuator and transmission combination does not match the human wrist in maximum speed. While human wrist speeds are currently too fast for a prosthetic hand user to control (see Section IIC) and thus not necessary in this prosthesis, if matching human muscle capabilities at the scale of forearm muscles were desirable, a substantial improvement in power density and specific power would be required in order to match this performance.

The weight of the actuators and transmissions means that approximately half of the prosthesis' weight is used for other purposes such as critical mechanical components (e.g. the *guide rail*, *base plate*, and *universal and spherical joints*). This is relatively high for a prosthesis and likely high relative to the human forearm and wrist. There is therefore potential for it to be substantially reduced through design changes including more custom rather than off-the-shelf components (e.g. the *universal* and *spherical joints*) rated specifically for the target specifications, better material selection (e.g. high performance plastics or composites with higher strength-to-density ratios than metals), and improved optimization.

VII. Conclusion and Future Work

The prosthesis presented in this paper is the first to achieve target performance in both speed and torque while achieving the target weight. It is therefore an important first step toward developing a prosthetic wrist that will ultimately meet user needs and be adopted by prosthetic hand users. Its performance is the result of using actuators and transmissions that have sufficient power density, torque density, and specific power as well as a mechanism that offers sufficient load bearing and transmission capability in a relatively small weight and close to sufficiently compact shape.

However, this prosthesis does not meet target dimensions because of the shape of commercially available BLDCs and planetary gearboxes, which are smaller in diameter and larger in length than would be ideal. We are currently investigating how to utilize BLDCs that are larger in diameter and smaller in length that would enable a collinear BLDC, gearbox, and ball screw. These BLDCs would also naturally be more torque dense (although potentially at the cost of lower specific power), reducing the size, weight, and number of stages for the planetary gearbox and thereby increasing its efficiency. Options such as drone motors have been utilized in prosthetic legs [165] and may offer promise in prosthetic wrists as well. If a BLDC and planetary gearbox could be sufficiently shorter in length to be collinear to the ball screw, it would lead to a substantially more compact prosthesis. RoM is similarly limited by the RoM of commercially available spherical joints, which can be improved through the integration of smaller custom joints.

In its current form, this prosthesis also lacks the requisite integrated motor drivers and controllers needed to be used in any practical scenario. However, multiple prostheses have demonstrated the feasibility of integrating custom electronic components into a prosthesis for minimal additional size or weight [13], [102], [103]. Finally, it is also critical to include P/S in any prosthetic wrist. While the dimensional constraints available for P/S are very different than for the prosthesis presented in this paper, the same actuator and transmission considerations used to achieve both sufficient speed and torque should be reflected in the mechanism selection and overall design. Without these considerations, it is unlikely that P/S could be achieved with sufficient specifications.

Acknowledgements

We would like to thank Megan Diemer and Alicia Davis for their contributions in providing feedback on the prosthesis. We would also like to thank Kent Pruss, Charlie Bradley, and Jonathon Yenkel for their contributions in fabricating the prosthesis prototype.

References

[1] C. W. Heckathorne, "Upper-Limb Prosthetics: Components for Adult Externally Powered Systems," in *Atlas of Limb Prosthetics: Surgical, Prosthetic, and Rehabilitation Principles*, 2nd ed., Rosemont, IL: Academy of Orthopedic Surgeons, 1992.

[2] R. F. Weir, "The Design of Artificial Arms and Hands for Prosthetic Applications," in *Standard Handbook of Biomedical Engineering and Design*, M. Kutz, Ed. New York: McGraw-Hill, 2003, pp. 32.1-32.59.

[3] J. T. Belter, J. L. Segil, A. M. Dollar, and R. F. Weir, "Mechanical design and performance specifications of anthropomorphic prosthetic hands: A review," *J. Rehabil. Res. Dev.*, vol. 50, no. 5, pp. 599–618, 2013, doi: 10.1682/JRRD.2011.10.0188.

[4] C. Piazza, G. Grioli, M. G. Catalano, and A. Bicchi, "A Century of Robotic Hands," *Annu. Rev. Control. Robot. Auton. Syst.*, vol. 2, no. 1, pp. 1–32, May 2019, doi: 10.1146/annurev-control-060117-105003.

[5] I. Vujaklija, D. Farina, and O. C. Aszmann, "New developments in prosthetic arm systems," *Orthopedic Research and Reviews*, vol. 8. Dove Medical Press Ltd., pp. 31–39, 07-Jul-2016, doi: 10.2147/ORR.S71468.

[6] J. ten Kate, G. Smit, and P. Breedveld, "3D-printed upper limb prostheses: a review," *Disability and Rehabilitation: Assistive Technology*, vol. 12, no. 3. Taylor and Francis Ltd, pp. 300–314, 03-Apr-2017, doi: 10.1080/17483107.2016.1253117.

[7] V. Mendez, F. Iberite, S. Shokur, and S. Micera, "Current Solutions and Future Trends for Robotic Prosthetic Hands," *Annu. Rev. Control. Robot. Auton. Syst.*, vol. 4, no. 1, pp. 595–627, 2021, doi: 10.1146/annurev-control-071020-104336.

[8] R. Damerla, Y. Qiu, T. M. Sun, and S. Awtar, "A Review of the Performance of Extrinsically Powered Prosthetic Hands," *IEEE Trans. Med. Robot. Bionics*, vol. 3, no. 3, pp. 640–660, Jul. 2021, doi: 10.1109/TMRB.2021.3100612.

[9] N. M. Bajaj, A. J. Spiers, and A. M. Dollar, "State of the Art in Artificial Wrists: A Review of Prosthetic and Robotic Wrist Design," *IEEE Trans. Robot.*, vol. 35, no. 1, pp. 261–277, Feb. 2019, doi: 10.1109/TRO.2018.2865890.

[10] "Mobius Bionics LUKE Arm Product Specification Sheet," Mobius Bionics, Manchester, NH, USA. [Online]. Available: https://www.mobiusbionics.com/luke-arm/

[11] L. Resnik, S. L. Klinger, and K. Etter, "The DEKA Arm: Its features, functionality, and evolution during the veterans affairs study to optimize the DEKA Arm," *Prosthet. Orthot. Int.*, vol. 38, no. 6, pp. 492–504, Dec. 2014, doi: 10.1177/0309364613506913.

[12] C. O. Evans *et al.*, "Arm Prosthetic Device," U.S. Patent 8,979,943 B2, 2015.

[13] M. S. Johannes *et al.*, "The modular prosthetic limb," in *Wearable Robotics: Systems and Applications*, Elsevier, 2020, pp. 393–444.

[14] K. Ziegler-Graham, E. J. MacKenzie, P. L. Ephraim, T. G. Travison, and R. Brookmeyer, "Estimating the Prevalence of Limb Loss in the United States: 2005 to 2050," *Arch. Phys. Med. Rehabil.*, vol. 89, no. 3, pp. 422–429, Mar. 2008, doi: 10.1016/j.apmr.2007.11.005.

[15] F. Cordella *et al.*, "Literature Review on Needs of Upper Limb Prosthesis Users," *Front. Neurosci.*, vol. 0, no. MAY, p. 209, 2016, doi: 10.3389/FNINS.2016.00209.

[16] I. Jeon *et al.*, "Trends in the incidence of work-related traumatic limb amputations in South Korea from 2004 to 2013:," *Prosthet. Orthot. Int.*, vol. 43, no. 4, pp. 409–417, Mar. 2019, doi: 10.1177/0309364619838356.

[17] M. Moini, M. R. Rasouli, A. Khaji, F. Farshidfar, and P. Heidari, "Patterns of extremity traumas leading to amputation in Iran: results of Iranian National Trauma Project," *Chinese J. Traumatol. (English Ed.)*, vol. 12, no. 2, pp. 77–80, Apr. 2009, doi: 10.3760/CMA.J.ISSN.1008-1275.2009.02.003.

[18] L. Resnik, J. Cancio, S. Klinger, G. Latlief, N. Sasson, and L. Smurr-Walters, "Predictors of retention and attrition in a study of an advanced upper limb prosthesis: implications for adoption of the DEKA Arm," *Disabil. Rehabil. Assist. Technol.*, vol. 13, no. 2, pp. 206–210, Feb. 2018,

doi: 10.1080/17483107.2017.1304585.

[19] L. V. Mcfarland, S. L. H. Winkler, A. W. Heinemann, M. Jones, and A. Esquenazi, "Unilateral upper-limb loss: Satisfaction and prosthetic-device use in veterans and servicemembers from Vietnam and OIF/OEF conflicts," *J. Rehabil. Res. Dev.*, vol. 47, no. 4, pp. 299–316, 2010, doi: 10.1682/JRRD.2009.03.0027.

[20] E. Biddiss and T. Chau, "Upper limb prosthesis use and abandonment: A survey of the last 25 years," *Prosthet. Orthot. Int.*, vol. 31, no. 3. SAGE PublicationsSage UK: London, England, pp. 236–257, 23-Sep-2007, doi: 10.1080/03093640600994581.

[21] L. Resnik, S. Ekerholm, M. Borgia, and M. A. Clark, "A national study of Veterans with major upper limb amputation: Survey methods, participants, and summary findings," *PLoS One*, vol. 14, no. 3, Mar. 2019, doi: 10.1371/journal.pone.0213578.

[22] E. Biddiss, D. Beaton, and T. Chau, "Consumer design priorities for upper limb prosthetics," *Disabil. Rehabil. Assist. Technol.*, vol. 2, no. 6, pp. 346–357, 2007, doi: 10.1080/17483100701714733.

[23] A. Chadwell *et al.*, "Upper limb activity in myoelectric prosthesis users is biased towards the intact limb and appears unrelated to goal-directed task performance," *Sci. Reports*, vol. 8, no. 1, pp. 1–12, Jul. 2018, doi: 10.1038/s41598-018-29503-6.

[24] A. J. Spiers, J. Cochran, L. Resnik, and A. M. Dollar, "Quantifying Prosthetic and Intact Limb Use in Upper Limb Amputees via Egocentric Video: An Unsupervised, At-Home Study," *IEEE Trans. Med. Robot. Bionics*, vol. 3, no. 2, pp. 463–484, 2021, doi: 10.1109/TMRB.2021.3072253.

[25] L. E. Jones and J. H. Davidson, "Save that arm: a study," *Prosthet. Orthot. Int.*, vol. 23, pp. 55–58, 1999.

[26] D. Datta, K. Selvarajah, and N. Davey, "Functional outcome of patients with proximal upper limb deficiency - Acquired and congenital," *Clin. Rehabil.*, vol. 18, no. 2, pp. 172–177, 2004, doi: 10.1191/0269215504cr716oa.

[27] C. R. Gambrell, "Overuse Syndrome and the Unilateral Upper Limb Amputee: Consequences and Prevention," *J. Prosthetics Orthot.*, vol. 20, no. 3, pp. 126–132, Jul. 2008, doi: 10.1097/JPO.0b013e31817ecb16.

[28] K. Østlie, R. J. Franklin, O. H. Skjeldal, A. Skrondal, and P. Magnus, "Musculoskeletal pain and overuse syndromes in adult acquired major upper-limb amputees," *Arch. Phys. Med. Rehabil.*, vol. 92, no. 12, pp. 1967-1973.e1, 2011, doi: 10.1016/j.apmr.2011.06.026.

[29] L. C. Smail, C. Neal, C. Wilkins, and T. L. Packham, "Comfort and function remain key factors in upper limb prosthetic abandonment: findings of a scoping review," *Disabil. Rehabil. Assist. Technol.*, 2020, doi: 10.1080/17483107.2020.1738567.

[30] S. M. Engdahl, B. P. Christie, B. Kelly, A. Davis, C. A. Chestek, and D. H. Gates, "Surveying the interest of individuals with upper limb loss in novel prosthetic control techniques," *J. Neuroeng. Rehabil.*, vol. 12, no. 1, Jun. 2015, doi: 10.1186/s12984-015-0044-2.

[31] C. Pylatiuk, S. Schulz, and L. Döderlein, "Results of an internet survey of myoelectric prosthetic hand users," *Prosthet. Orthot. Int.*, vol. 31, no. 4, pp. 362–370, Dec. 2007, doi: 10.1080/03093640601061265.

[32] L. Resnik, H. Benz, M. Borgia, and M. A. Clark, "Patient perspectives on benefits and risks of implantable interfaces for upper limb prostheses: a national survey," *Expert Rev. Med. Devices*, vol. 16, no. 6, 2019, doi: 10.1080/17434440.2019.1619453.

[33] M. Espinosa and D. Nathan-Roberts, "Understanding Prosthetic Abandonment," *Proc. Hum. Factors Ergon. Soc. Annu. Meet.*, vol. 63, no. 1, pp. 1644–1648, Nov. 2019, doi: 10.1177/1071181319631508.

[34] B. Peerdeman *et al.*, "Myoelectric forearm prostheses: State of the art from a user-centered perspective," *J. Rehabil. Res. Dev.*, vol. 48, no. 6, p. 719, Jan. 2011, doi: 10.1682/JRRD.2010.08.0161.

[35] A. J. Metzger, A. W. Dromerick, R. J. Holley, and P. S. Lum, "Characterization of compensatory trunk movements during prosthetic upper limb reaching tasks," *Arch. Phys. Med. Rehabil.*, vol. 93, no. 11, pp. 2029–2034, 2012, doi: 10.1016/j.apmr.2012.03.011.

[36] M. J. Major, R. L. Stine, C. W. Heckathorne, S. Fatone, and S. A. Gard, "Comparison of range-of-motion and variability in upper body movements between transradial prosthesis users and able-bodied controls when executing goal-oriented tasks," *J. Neuroeng. Rehabil.*, vol. 11, pp. 1–10, 2014, doi: 10.1186/1743-0003-11-132.

[37] A. Hussaini, A. Zinck, and P. Kyberd, "Categorization of compensatory motions in transradial myoelectric prosthesis users," *Prosthet. Orthot. Int.*, vol. 41, no. 3, pp. 286–293, 2017, doi: 10.1177/0309364616660248.

[38] S. L. Carey, M. Jason Highsmith, M. E. Maitland, and R. V. Dubey, "Compensatory movements of transradial prosthesis users during common tasks," *Clin. Biomech.*, vol. 23, no. 9, pp. 1128–1135, 2008, doi: 10.1016/j.clinbiomech.2008.05.008.

[39] F. Montagnani, M. Controzzi, and C. Cipriani, "Is it Finger or Wrist Dexterity That is Missing in Current Hand Prostheses?," *IEEE Trans. Neural Syst. Rehabil. Eng.*, vol. 23, no. 4, pp. 600–609, 2015, doi: 10.1109/TNSRE.2015.2398112.

[40] A. J. Spiers, Y. Gloumakov, and A. M. Dollar, "Examining the Impact of Wrist Mobility on Reaching Motion Compensation Across a Discretely Sampled Workspace," in *Proceedings of the IEEE RAS and EMBS International Conference on Biomedical Robotics and Biomechatronics, Biorob 2018*, 2018, pp. 819–826, doi: 10.1109/BIOROB.2018.8487871.

[41] M. Deijs, R. M. Bongers, N. D. M. Ringeling-Van Leusen, and C. K. Van Der Sluis, "Flexible and static wrist units in upper limb prosthesis users: Functionality scores, user satisfaction and compensatory movements," *J. Neuroeng. Rehabil.*, vol. 13, pp. 1–13, 2016, doi: 10.1186/s12984-016-0130-0.

[42] G. Kanitz, F. Montagnani, M. Controzzi, and C. Cipriani, "Compliant Prosthetic Wrists Entail More Natural Use Than Stiff Wrists during Reaching, Not (Necessarily) during Manipulation," *IEEE Trans. Neural Syst. Rehabil. Eng.*, vol. 26, no. 7, pp. 1407–1413, 2018, doi: 10.1109/TNSRE.2018.2847565.

[43] P. J. Kyberd, "The influence of passive wrist joints on the functionality of prosthetic hands," *Prosthet. Orthot. Int.*, vol. 36, no. 1, pp. 33–38, 2012, doi: 10.1177/0309364611426905.

[44] T. Bertels, T. Schmalz, and E. Ludwigs, "Objectifying the Functional Advantages of Prosthetic Wrist Flexion," *J. Prosthetics Orthot.*, vol. 21, no. 2, pp. 74–78, Apr. 2009, doi: 10.1097/JPO.0b013e3181a10f46.

[45] H. H. Sears, E. Iversen, S. Archer, and T. Jacobs, "Wrist Innovations To Improve Function of Electric Terminal Devices," in *Proceedings of the 2008 MyoElectric Controls/Powered Prosthetics Symposium*, 2008, pp. 1–4.

[46] "MC Standard and ProWrist Rotators Fact Sheet," Fillauer, Chattanooga, TN, USA. [Online]. Available: https://fillauer.com/wp-content/uploads/2020/08/1910062-FACT-SHEET-Wrist-Rotator-Rev-E-08-26-2020.pdf

[47] "Ottobock Electric Wrist Rotator Flyer," Ottobock, Duderstadt, DEU. [Online]. Available: https://shop.ottobock.us/Prosthetics/Upper-Limb-Prosthetics/Myo-Hands-and-Components/Myo-Wrist-Units-and-Rotation/Electric-Wrist-Rotator/p/10S17#product-documents-section

[48] "i-Limb Wrist Technical Manual," Össur, Reykjavik, ISL. [Online]. Available: https://training.touchbionics.com/pdfs/1421_002_i-Limb_Wrist_Technical_Manual.pdf

[49] H. Gill, "Systems and Methods for Prosthetic Wrist Rotation," U.S. Patent 10,369,024 B2, 2019.

[50] "Motion Control Powered Flexion Wrist Flyer," Fillauer, Chattanooga, TN, USA. [Online]. Available: https://fillauer.com/products/mc-powered-flexion-wrist/

[51] E. K. Iversen, J. Christensen, and G. J. Jacobs, "Powered Prosthetic Flexion Device," U.S. Patent 2020/0375761 A1, 2020.

[52] B. Hirt, H. Seyhan, M. Wagner, and R. Zumbasch, "Wrist and Movement Axes," in *Hand and Wrist Anatomy and Biomechanics: A Comprehensive Guide*, 1st ed., Stuttgart, Germany, 2017, pp. 10–47.

[53] B. Hirt, H. Seyhan, M. Wagner, and R. Zumbasch, "Anatomy and Functional Anatomy of the Hand," in *Hand and Wrist Anatomy and Biomechanics: A Comprehensive Guide*, 1st ed., Stuttgart, Germany, 2017, pp. 2–9.

[54] B. Hirt, H. Seyhan, M. Wagner, and R. Zumbasch, "Structure and Function of the Finger Joints," in *Hand and Wrist Anatomy and Biomechanics: A Comprehensive Guide*, 1st ed., Stuttgart, Germany: Thieme, 2017, pp. 66–80.

[55] J. W. Garrett, "Anthropometry of the Air Force Female Hand," Mar. 1970.

[56] J. W. Garrett, "Anthropometry of the Hands of Male Air Force Flight Personnel," 1970.

[57] R. J. Marley and M. R. Thomson, "Isokinetic Strength Characteristics in Wrist Flexion and Extension," *Int. J. Ind. Ergon.*, vol. 25, no. 6, pp. 633–643, 2000.

[58] T. Xia and L. A. Frey-Law, "Wrist joint torque-angle-velocity performance capacity envelope evaluation and modelling," *Int. J. Hum. Factors Model. Simul.*, vol. 5, no. 1, pp. 33–52, 2015.

[59] T. M. Greiner, "Hand Anthropometry of U.S. Army Personnel," 1991.

[60] R. M. White, "Comparative Anthropometry Of The Hand," 1981.

[61] C. C. Gordon *et al.*, "2012 Anthropometric Survey of U.S. Army Personnel: Methods and Summary Statistics," 2014.

[62] R. W. Schoenmarklin and W. S. Marras, "Dynamic capabilities of the wrist joint in industrial workers," *Int. J. Ind. Ergon.*, vol. 11, no. 3, pp. 207–224, 1993, doi: 10.1016/0169-8141(93)90109-Q.

[63] J. T. Barter, I. Emanuel, and B. Truett, “A statistical evaluation of joint range data,” 1957.
[64] A. R. Bonebrake, J. E. Fernandez, R. J. Marley, J. B. Dahalan, and K. J. Kilmer, “A treatment for carpal tunnel syndrome: Evaluation of objective and subjective measures,” *J. Manipulative Physiol. Ther.*, vol. 13, no. 9, pp. 507–520, 1990.
[65] J. M. Soucie *et al.*, “Range of motion measurements: Reference values and a database for comparison studies,” *Haemophilia*, vol. 17, no. 3, pp. 500–507, 2011, doi: 10.1111/j.1365-2516.2010.02399.x.
[66] M. M. Marshall, J. R. Mozrall, and J. E. Shealy, “The effects of complex wrist and forearm posture on wrist range of motion,” *Hum. Factors*, vol. 41, no. 2, pp. 205–213, 1999, doi: 10.1518/001872099779591178.
[67] D. C. Boone and S. P. Azen, “Normal range of motion of joints in male subjects,” *J. Bone Jt. Surg.*, vol. 61, no. 5, pp. 756–759, 1979, doi: 10.2106/00004623-197961050-00017.
[68] M. Sardelli, R. Z. Tashjian, and B. A. MacWilliams, “Functional elbow range of motion for contemporary tasks,” *J. Bone Jt. Surg.*, vol. 93, no. 5, pp. 471–477, 2011, doi: 10.2106/JBJS.I.01633.
[69] B. F. Morrey, L. J. Askew, K. N. An, and E. Y. Chao, “A biomechanical study of normal functional elbow motion,” *J. Bone Jt. Surg.*, vol. 63, no. 6, pp. 872–877, 1981, doi: 10.2106/00004623-198163060-00002.
[70] S. Henmi, K. Yonenobu, T. Masatomi, and K. Oda, “A biomechanical study of activities of daily living using neck and upper limbs with an optical three-dimensional motion analysis system,” *Mod. Rheumatol.*, vol. 16, pp. 289–293, 2006, doi: 10.1007/s10165-006-0499-x.
[71] J. Aizawa *et al.*, “Three-dimensional motion of the upper extremity joints during various activities of daily living,” *J. Biomech.*, vol. 43, no. 15, pp. 2915–2922, 2010, doi: 10.1016/j.jbiomech.2010.07.006.
[72] D. L. Nelson, M. A. Mitchell, P. G. Groszewski, S. L. Pennick, and P. R. Manske, “Wrist Range of Motion in Activities of Daily Living,” *Adv. Biomech. Hand Wrist*, pp. 329–334, 1994, doi: 10.1007/978-1-4757-9107-5_29.
[73] D. H. Gates, L. S. Walters, J. Cowley, J. M. Wilken, and L. Resnik, “Range of motion requirements for upper-limb activities of daily living,” *Am. J. Occup. Ther.*, vol. 70, no. 1, pp. 1–10, 2016, doi: 10.5014/ajot.2016.015487.
[74] J. Ryu, W. P. Cooney, L. J. Askew, K. N. An, and E. Y. S. Chao, “Functional ranges of motion of the wrist joint,” *J. Hand Surg. Am.*, vol. 16, no. 3, pp. 409–419, 1991, doi: 10.1016/0363-5023(91)90006-W.
[75] M. Doğan *et al.*, “Functional range of motion in the upper extremity and trunk joints: Nine functional everyday tasks with inertial sensors,” *Gait Posture*, vol. 70, pp. 141–147, 2019, doi: 10.1016/j.gaitpost.2019.02.024.
[76] W. Dempster and G. Gaughran, “Properties of Body Sements Based on Size and Weight,” *Am. J. Anat.*, vol. 120, pp. 33–54, 1967.
[77] S. Plagenhoef, F. Gaynor Evans, and T. Abdelnour, “Anatomical Data for Analyzing Human Motion,” *Res. Quarterly Exerc. Sport*, vol. 54, no. 2, pp. 169–178, 1983, doi: 10.1080/02701367.1983.10605290.
[78] C. E. Clauser, J. T. McConville, and J. W. Young, “Weight, Volume, and Center of Mass of Segments of the Human Body,” *Natl. Tech. Inf. Serv.*, pp. 1–101, 1969, doi: AMRL-TR- 69-70 (AD 710 622).
[79] P. de Leva, “Adjustments to Zatsiorsky-Selyanov’s Segment Inertia Parameters,” *J. Biomech.*, vol. 29, no. 9, pp. 1223–1230, 1996.
[80] J. Shealy and W. Latko, “Effects of Mass on Wrist Velocities and Accelerations,” in *Proceedings of the Human Factors Society 36th Annual Meeting*, 1992, pp. 761–764.
[81] H. Ida, K. Fukuhara, S. Kusubori, and M. Ishii, “A study of kinematic cues and anticipatory performance in tennis using computational manipulation and computer graphics,” *Behav. Res. Methods*, vol. 43, pp. 781–790, 2011, doi: 10.3758/s13428-011-0084-x.
[82] S. K. Charles and N. Hogan, “Dynamics of wrist rotations,” *J. Biomech.*, vol. 44, no. 4, pp. 614–621, 2011, doi: 10.1016/j.jbiomech.2010.11.016.
[83] G. Å. Hansson *et al.*, “Physical workload in various types of work: Part I. Wrist and forearm,” *Int. J. Ind. Ergon.*, vol. 39, no. 1, pp. 221–233, 2009, doi: 10.1016/j.ergon.2008.04.003.
[84] L. W. O’Sullivan and T. J. Gallwey, “Forearm torque strengths and discomfort profiles in pronation and supination,” *Ergonomics*, vol. 48, no. 6, pp. 703–721, 2005, doi: 10.1080/00140130500070954.
[85] J. Matsuoka, R. A. Berger, L. J. Berglund, and K. An, “An Analysis of of the Forearm Under Resisted Forearm Rotation in Normal Subjects,” *J. Hand Surg. Am.*, vol. 31A, no. 5, pp. 801–805, 2006.
[86] P. Axelsson, P. Fredrikson, A. Nilsson, J. K. Andersson, and J. Kärrholm, “Forearm Torque and Lifting Strength: Normative Data,” *J. Hand Surg. Am.*, vol. 43, no. 7, pp. 677.e1-677.e17, 2018, doi: 10.1016/j.jhsa.2017.12.022.
[87] Y. Yoshii, H. Yuine, O. Kazuki, W. lin Tung, and T. Ishii, “Measurement of wrist flexion and extension torques in different forearm positions,” *Biomed. Eng. Online*, vol. 14, pp. 1–10, 2015, doi: 10.1186/s12938-015-0110-9.
[88] V. Decostre *et al.*, “Wrist flexion and extension torques measured by highly sensitive dynamometer in healthy subjects from 5 to 80 years,” *BMC Musculoskelet. Disord.*, vol. 16, pp. 1–10, 2015, doi: 10.1186/s12891-015-0458-9.
[89] A. Zinck, Ø. Stavdahl, E. Biden, and P. J. Kyberd, “Design of a compact, reconfigurable, prosthetic wrist,” *Appl. Bionics Biomech.*, vol. 9, pp. 117–124, 2012, doi: 10.3233/ABB-2011-0043.
[90] K. R. S. Holzbaur, W. M. Murray, G. E. Gold, and S. L. Delp, “Upper limb muscle volumes in adult subjects,” *J. Biomech.*, vol. 40, no. 4. pp. 742–749, 2007, doi: 10.1016/j.jbiomech.2006.11.011.
[91] I. W. Hunter and S. Lafontaine, “Comparison of muscle with artificial actuators,” in *Technical Digest- IEEE Solid-State Sensor and Actuator Workshop*, 1992, pp. 178–185, doi: 10.1109/solsen.1992.228297.
[92] R. Damerla and S. Awtar, “Constraint-Based Analysis of Parallel Kinematic Articulated Wrist Mechanisms,” *J. Mech. Robot.*, vol. 13, no. 3, Jun. 2021, doi: 10.1115/1.4049947.
[93] Y. D. Patel and P. M. George, “Parallel Manipulators Applications-A Survey,” *Mod. Mech. Eng.*, vol. 2, pp. 57–64, 2012, doi: 10.4236/mme.2012.23008.
[94] G. Pritschow, “Parallel Kinematic Machines (PKM) – Limitations and New Solutions,” *Ann. of the CIRP*, vol. 49, no. 1, pp. 275–280, Jan. 2000, doi: 10.1016/S0007-8506(07)62945-X.
[95] J. L. Pons *et al.*, “The MANUS-HAND * Dextrous Robotics Upper Limb Prosthesis: Mechanical and Manipulation Aspects,” *Auton. Robots*, vol. 16, pp. 143–163, 2004.
[96] M. L. Davidson, “Development of a Novel Prosthetic Wrist Device Incorporating the Dart Thrower’s Motion,” Ph.D. dissertation, Bioeng., University of Colorado at Denver, Denver, CO, USA, 2017.
[97] G. Lee, G. Y. Hong, and Y. Choi, “Tendon-driven compliant prosthetic wrist consisting of three rows based on the concept of tensegrity structure,” *IEEE Robot. Autom. Lett.*, vol. 6, no. 2, pp. 3956–3963, 2021, doi: 10.1109/LRA.2021.3067237.
[98] P. J. Kyberd *et al.*, “Two-degree-of-freedom powered prosthetic wrist,” *J. Rehabil. Res. Dev.*, vol. 48, no. 6, pp. 609–618, 2011, doi: 10.1682/JRRD.2010.07.0137.
[99] N. M. Bajaj and A. M. Dollar, “Design and Preliminary Evaluation of a 3-DOF Powered Prosthetic Wrist Device,” in *Proceedings of the IEEE RAS and EMBS International Conference on Biomedical Robotics and Biomechatronics*, 2018, pp. 119–125, doi: 10.1109/BIOROB.2018.8487192.
[100] R. Mahmoud, A. Ueno, and S. Tatsumi, “An assistive tele-operated anthropomorphic robot hand: Osaka city university hand II,” in *2011 6th ACM/IEEE International Conference on Human-Robot Interaction (HRI)*, 2011, pp. 85–92, doi: 10.1145/1957656.1957677.
[101] N. A. Abd Razak, N. A. Abu Osman, H. Gholizadeh, and S. Ali, “Development and performance of a new prosthesis system using ultrasonic sensor for wrist movements: A preliminary study,” *Biomed. Eng. Online*, vol. 13, pp. 1–14, 2014, doi: 10.1186/1475-925X-13-49.
[102] J. Lipsey and J. Sensinger, “Modular and lightweight myoelectric prosthesis components and related methods,” U.S. Patent 2019/0380846 A1, 2019.
[103] T. Lenzi, J. Lipsey, and J. W. Sensinger, “The RIC Arm - A Small Anthropomorphic Transhumeral Prosthesis,” *IEEE/ASME Trans. Mechatronics*, vol. 21, no. 6, pp. 2660–2671, 2016, doi: 10.1109/TMECH.2016.2596104.
[104] N. R. Olsen *et al.*, “An Adaptable Prosthetic Wrist Reduces Subjective Workload,” *bioRxiv*, Oct. 2019, doi: 10.1101/808634.
[105] C. Roose, “Two-Degree-of-Freedom Pneumatically Powered Wrist Prosthesis,” Delft University of Technology, Delft, Netherlands, 2014.
[106] H. Takeda, N. Tsujiuchi, T. Koizumi, H. Kan, M. Hirano, and Y. Nakamura, “Development of prosthetic arm with pneumatic prosthetic hand and tendon-driven wrist,” in *Proceedings of the 31st Annual International Conference of the IEEE Engineering in Medicine and Biology Society: Engineering the Future of Biomedicine, EMBC 2009*, 2009, pp. 5048–5051, doi: 10.1109/IEMBS.2009.5333668.
[107] M. Hioki *et al.*, “Design and control of electromyogram prosthetic hand with high grasping force,” in *2011 IEEE International Conference on Robotics and Biomimetics, ROBIO 2011*, 2011, pp. 1128–1133, doi: 10.1109/ROBIO.2011.6181439.
[108] H. Kawasaki, T. Mouri, T. Hara, and H. Shimomura, “Humanoid Electric Hand,” U.S. Patent 8,747,486 B2, 2014.
[109] K. B. Fite, T. J. Withrow, X. Shen, K. W. Wait, J. E. Mitchell, and M.

Goldfarb, “A gas-actuated anthropomorphic prosthesis for transhumeral amputees,” *IEEE Trans. Robot.*, vol. 24, no. 1, pp. 159–169, Feb. 2008, doi: 10.1109/TRO.2007.914845.

[110] S. K. Kundu and K. Kiguchi, “Development of a 5 DOF prosthetic arm for above elbow amputees,” in *Proceedings of 2008 IEEE International Conference on Mechatronics and Automation, ICMA 2008*, 2008, pp. 207–212, doi: 10.1109/ICMA.2008.4798753.

[111] F. Zajac, “Muscle and tendon: properties, models, scaling, and application to biomechanics and motor control.,” *Crit. Rev. Biomed. Eng.*, vol. 17, no. 4, pp. 359–410, 1989.

[112] “Pneumatic cylinders | McMaster-Carr.” [Online]. Available: https://www.mcmaster.com/pneumatic-cylinders/.

[113] W. Liang, H. Liu, K. Wang, Z. Qian, L. Ren, and L. Ren, “Comparative study of robotic artificial actuators and biological muscle,” *Adv. Mech. Eng.*, vol. 12, no. 6, p. 168781402093340, Jun. 2020, doi: 10.1177/1687814020933409.

[114] I. W. Hunter, J. M. Hollerbach, and J. Ballantyne, “A comparative analysis of actuator technologies for robotics,” *Robot. Rev. 2*, pp. 299–342, 1991.

[115] A. Nespoli, S. Besseghini, S. Pittaccio, E. Villa, and S. Viscuso, “The high potential of shape memory alloys in developing miniature mechanical devices: A review on shape memory alloy mini-actuators,” *Sensors Actuators A Phys.*, vol. 158, no. 1, pp. 149–160, Mar. 2010, doi: 10.1016/J.SNA.2009.12.020.

[116] H. Stroud and D. Hartl, “Shape memory alloy torsional actuators: a review of applications, experimental investigations, modeling, and design,” *Smart Mater. Struct.*, vol. 29, no. 11, p. 113001, Oct. 2020, doi: 10.1088/1361-665X/ABBB12.

[117] J. Mohd Jani, M. Leary, A. Subic, and M. A. Gibson, “A review of shape memory alloy research, applications and opportunities,” *Mater. Des.*, vol. 56, pp. 1078–1113, Apr. 2014, doi: 10.1016/J.MATDES.2013.11.084.

[118] J. Mohd Jani, M. Leary, and A. Subic, “Designing shape memory alloy linear actuators: A review:,” *http://dx.doi.org/10.1177/1045389X16679296*, vol. 28, no. 13, pp. 1699–1718, Dec. 2016, doi: 10.1177/1045389X16679296.

[119] K. Andrianesis and A. Tzes, “Development and Control of a Multifunctional Prosthetic Hand with Shape Memory Alloy Actuators,” *J. Intell. Robot. Syst.*, vol. 78, pp. 257–289, May 2015, doi: 10.1007/s10846-014-0061-6.

[120] “Cedrat Technologies Product Catalog,” Cedrat Technologies, Meylan, France. [Online]. Available: https://www.cedrat-technologies.com/en/download-1.html

[121] “PiezoMove High-Stiffness Linear Piezo Actuator,” PI USA, Auburn, MA, USA. [Online]. Available: https://www.pi-usa.us/en/products/piezo-actuators-stacks-benders-tubes/p-602-piezomove-high-stiffness-linear-piezo-actuator-202700/#specification

[122] “DSM Piezo Actuators,” Dynamic Structures & Materials, LLC, Franklin, TN, USA. [Online]. Available: https://www.dynamic-structures.com/piezo-actuators

[123] A. Shafik and R. Ben Mrad, “Piezoelectric Motor Technology: A Review,” *Nanopositioning Technol. Fundam. Appl.*, pp. 33–59, Jan. 2016, doi: 10.1007/978-3-319-23853-1_2.

[124] G. Rui Zhang, P. Lochmatter, A. Kunz, G. M. Kovacs, R. Zhang, and G. Kovacs, “Spring roll dielectric elastomer actuators for a portable force feedback glove,” *https://doi.org/10.1117/12.658524*, vol. 6168, no. 22, pp. 505–516, Mar. 2006, doi: 10.1117/12.658524.

[125] R. W. Jones *et al.*, “An arm wrestling robot driven by dielectric elastomer actuators,” *Smart Mater. Struct.*, vol. 16, no. 2, p. S306, Mar. 2007, doi: 10.1088/0964-1726/16/2/S16.

[126] T. Lu, C. Ma, and T. Wang, “Mechanics of dielectric elastomer structures: A review,” *Extrem. Mech. Lett.*, vol. 38, p. 100752, Jul. 2020, doi: 10.1016/J.EML.2020.100752.

[127] T. Lu, C. Chiang Foo, J. Huang, J. Zhu, and Z. Suo, “Highly deformable actuators made of dielectric elastomers clamped by rigid rings,” *J. Appl. Phys*, vol. 115, no. 18, p. 184105, May 2014, doi: 10.1063/1.4876722.

[128] G. Kovacs, L. Düring, S. Michel, and G. Terrasi, “Stacked dielectric elastomer actuator for tensile force transmission,” *Sensors Actuators A: Physical*, vol. 155, no. 2, pp. 299–307, Oct. 2009, doi: 10.1016/J.SNA.2009.08.027.

[129] D. Rossi, D. F. Carpi, D. De Rossi, and F. Carpi, “Contractile folded dielectric elastomer actuators,” *Proc. SPIE 6524, Electroactive Polymer Actuators and Devices (EAPAD) 2007*, vol. 6524, no. 4, pp. 127–139, Apr. 2007, doi: 10.1117/12.715594.

[130] M. Randazzo, R. Buzio, G. Metta, G. Sandini, and U. Valbusa, “Architecture for the semi-automatic fabrication and assembly of thin-film based dielectric elastomer actuators,” *Proc. SPIE 6927, Electroactive Polymer Actuators and Devices (EAPAD) 2008*, vol. 6927, pp. 739–748, Apr. 2008, doi: 10.1117/12.784981.

[131] P. Rothemund *et al.*, “HASEL Artificial Muscles for a New Generation of Lifelike Robots—Recent Progress and Future Opportunities,” *Adv. Mater.*, vol. 33, no. 19, p. 2003375, May 2021, doi: 10.1002/ADMA.202003375.

[132] Z. Yoder *et al.*, “Design of a High-Speed Prosthetic Finger Driven by Peano-HASEL Actuators,” *Front. Robot. AI*, vol. 7, p. 181, Nov. 2020, doi: 10.3389/FROBT.2020.586216/BIBTEX.

[133] N. Kellaris, V. G. Venkata, P. Rothemund, and C. Keplinger, “An analytical model for the design of Peano-HASEL actuators with drastically improved performance,” *Extrem. Mech. Lett.*, vol. 29, p. 100449, May 2019, doi: 10.1016/J.EML.2019.100449.

[134] R. Hinchet, H. Shea, R. Hinchet, and H. Shea, “High Force Density Textile Electrostatic Clutch,” *Adv. Mater. Technol.*, vol. 5, no. 4, p. 1900895, Apr. 2020, doi: 10.1002/ADMT.201900895.

[135] F. Claeyssen and N. Lhermet, “Actuators Based on Giant Magnetostrictive Materials,” in *ACTUATOR 2002, 8th International Conference on New Actuators*, 2002, pp. 148–153.

[136] G. Dai *et al.*, “A review of magnetostrictive iron–gallium alloys,” *Smart Mater. Struct.*, vol. 20, no. 4, p. 043001, Mar. 2011, doi: 10.1088/0964-1726/20/4/043001.

[137] N. Gabdullin and S. H. Khan, “Review of properties of magnetic shape memory (MSM) alloys and MSM actuator designs,” *J. Phys. Conf. Ser.*, vol. 588, no. 1, p. 012052, Feb. 2015, doi: 10.1088/1742-6596/588/1/012052.

[138] J. Tellinen, I. Suorsa, A. Jääskeläinen, I. Aaltio, and K. Ullakko, “Basic Properties of Magnetic Shape Memory Actuators,” in *ACTUATOR 2002, 8th International Conference on New Actuators*, 2002.

[139] “Maxon Selection Guide: 2019/2020,” Maxon Group, Sachseln, Switzerland. [Online]. Available: https://www.maxongroup.co.uk/maxon/view/news/The-new-maxon-catalogue-for-20192020

[140] “Faulhaber Drive Systems: 2018,” Faulhaber Micromo, Clearwater, FL, USA. [Online]. Available: https://pdf.directindustry.com/pdf/faulhaber-drive-systems-7023.html

[141] “Adamant Namiki Customized Actuator Catalog,” Adamant Namiki Precision Jewel Co., Tokyo, Japan. [Online]. Available: https://www.ad-na.com/en/product/dccorelessmotor/brushlessmotor.html

[142] “Brushless DC Motors From ElectroCraft,” ElectroCraft, Inc., Stratham, NH, USA. [Online]. Available: https://www.electrocraft.com/products/bldc/.

[143] “Moog Brushless Motors Overview,” Moog Inc., Elma, NY, USA. [Online]. Available: https://www.moog.com/content/sites/global/en/products/motors-servomotors/brushless-motors/.

[144] “MinebeaMitsumi Brushless Motors,” MinebeaMitsumi Inc., Tokyo, Japan. [Online]. Available: https://www.minebeamitsumi.eu/en/brushless-motor/.

[145] “Harmonic Drive General Catalog”, Harmonic Drive LLC, Beverly, MA, USA. [Online]. Available: https://www.harmonicdrive.net/downloads/catalogs

[146] “Cone Drive Harmonic Solutions Catalog,” Cone Drive, Traverse City, MI, USA. [Online]. Available: https://conedrive.com/resources/

[147] “GAM GSL Strain Wave Gearbox Catalog,” GAM, Prospect, IL, USA. [Online]. Available: https://www.gamweb.com/gsl-robotic-strain-wave-gearbox.html

[148] “DieQua Precision Cycloidal Reducers Catalog,” DieQua Corporation, Bloomingdale, IL, USA. [Online]. Available: https://diequa.com/catalog-downloads/

[149] “Nabtesco Precision Reduction Gear RV Catalog,” Nabtesco Motion Control, Inc., Farmington Hills, MI, USA. [Online]. Available: https://www.nabtescomotioncontrol.com/downloads/

[150] “KHK Worm Gear Pair Catalog,” Kohara Gear Industry Co., Ltd., Kawaguchi, Saitama, Japan. [Online]. Available: https://khkgears.net/new/worm_gear.html

[151] “SDP/SI Worms & Worm Gears Catalog,” Designatronics Inc., Hicksville, NY, USA. [Online]. Available: https://www.sdp-si.com/products/Gears/Index.php

[152] “Rush Gears Worm Gear Ratio & Torque Info,” Rush Gears Inc., Fort Washington, PA, USA. [Online]. Available: https://www.rushgears.com/tech-tools/worm-gear-ratios-and-torque.

[153] “KSS Standard Products of Ball Screws,” KSS Co., Ltd., Ohta-ku,

Tokyo, Japan. [Online]. Available: https://www.kssballscrew.com/us/download/download.html
[154] "NSK Ball Screws," NSK Ltd., Shinagawa-Ku, Tokyo, Japan. [Online]. Available: https://www.nsk.com/products/precisionmachine/ballscrew/
[155] "Thomson Ball Screws and Ball Splines," Thomson Industries, Inc., Radford, VA, USA. [Online]. Available: https://www.thomsonlinear.com/en/products/ball-screws#literature
[156] "TBI Motion Ball Screw Catalog," TBI Motion Technology Co., Ltd., New Taipei City, Taiwan. [Online]. Available: https://www.tbimotion.com.tw/en/product/Ball-Screw-SFK/ball-screw_SFK.html
[157] "Misumi Motion Systems Product Catalog," MISUMI Corporation, Schaumberg, IL, USA. [Online]. Available: https://us.misumi-ec.com/contents/company/about/
[158] "SDP/SI Timing belts, Pulleys, Chains and Sprockets Catalog," Designatronics Inc., Hicksville, NY, USA. [Online]. Available: https://www.sdp-si.com/products/Gears/Index.php
[159] "KSS Precision Lead Screws," KSS Co., Ltd., Ohta-ku, Tokyo, Japan. [Online]. Available: https://www.kssballscrew.com/us/download/download.html
[160] "Roller Chain," USA Roller Chain & Sprockets, Winter Garden, FL, USA. [Online]. Available: https://www.usarollerchain.com/Roller-Chain-s/2115.htm.
[161] S. Bai, X. Li, and J. Angeles, "A review of spherical motion generation using either spherical parallel manipulators or spherical motors," *Mech. Mach. Theory*, vol. 140, pp. 377–388, Oct. 2019, doi: 10.1016/J.MECHMACHTHEORY.2019.06.012.
[162] "Hand Chassis w/ Quick Disconnect Wrist." [Online]. Available: https://www.spshangerstore.com/hand-chassis-w-quick-disconnect-wrist.html.
[163] L. F. Bieg and G. L. Benavides, "Large displacement spherical joint," U.S. Patent 6,409,413 B1, 2002.
[164] N. M. Bajaj and A. M. Dollar, "Design of a Large Workspace Passive Spherical Joint via Contact Edge Design," *Proc. ASME Des. Eng. Tech. Conf.*, vol. 10, Nov. 2020, doi: 10.1115/DETC2020-22753.
[165] A. F. Azocar, L. M. Mooney, L. J. Hargrove, and E. J. Rouse, "Design and Characterization of an Open-Source Robotic Leg Prosthesis," *Proc. IEEE RAS EMBS Int. Conf. Biomed. Robot. Biomechatronics*, vol. 2018-August, pp. 111–118, Oct. 2018, doi: 10.1109/BIOROB.2018.8488057.